JOURNAL OF MECHANICS OF MATERIALS AND STRUCTURES
Vol. 4, No. 5, 2009

EVOLUTIONARY CONTROL OF STRUCTURALLY DAMAGED STEEL BUILDINGS USING AN OPTIMAL STATE TRANSITION FORMULATION

THOMAS L. ATTARD AND ROBIN E. DANSBY

An evolutionary gain formulation is proposed for minimizing the performance damage index of steel buildings subjected to earthquake forces. The gain formulation herein is used to develop the evolutionary control law of a control algorithm applied to inelastic systems. The optimal evolutionary gain is subsequently used to control building damages by satisfying desired performance objectives per time step "as needed". The performance objectives are defined for various "damage-safe" and elastic demands. When the structure responds in the post-yield (inelastic) state, the material is assumed to follow a kinematic rule for strain hardening, which consequently may redefine the performance objective window at each unload/reload response state (cyclic control).

A control nonlinear time-history analysis program, dubbed CONON, was developed to simulate the stress-strain responses of structural members and to compute the optimal control forces per time step. The minimization of the cost function is independent of weighing matrices, thus alleviating cumbersome calculations that also lack physical description. Instead, an iterative Riccati matrix is computed per time step and is used to generate the evolutionary gain for the system leading to an appropriate evolution of the state transition between time steps. The calculated control responses are compared to uncontrolled responses. The results are also compared using various methods of gain calculation by examining the force-deflection hysteresis plots, the strain energy dissipation in the structural members, and the member accelerations of a steel frame. The proposed optimal system shows an excellent capability to control the desired target responses and meet acceptable performance objectives.

1. Introduction

Performance-based structural engineering may be defined according to allowable damage performance levels (e.g., life safety or collapse prevention objectives [FEMA 2001]), or according to structural control theory. Control devices may be manufactured to utilize this latter control-based formulation to enable structures to respond elastically by providing damage-mitigation capability [Ohtori et al. 2004].

Structural control devices may be classified into three general categories: passive, active, and semiactive [Christenson and Emmons 2005]. Passive control is characterized by nonadaptive behavior. Such devices are typically designed for an expected earthquake and are unable to vary their resistance during a seismic event [Hart and Wong 2000]. Active and semiactive control devices, however, have the ability to adapt to the performance needs of a structure during an earthquake. Active control devices work by applying counterforces to reduce structural responses. Semiactive control devices require less power to operate [Christenson and Emmons 2005] and are able to apply resistive forces by effectively changing the stiffness and/ or damping in a structure thus reducing the structural responses.

Keywords: evolutionary structural dynamics, optimal control, evolutionary gain, plastic analysis, inelastic structures.

Passive base isolation and (passive) viscous damping as adopted by the Federal Emergency Management Association [FEMA 2001] and the International Building Code [IBC 2003] may provide viable and relatively inexpensive solutions toward mitigating seismic damages in buildings. However, certain long-period displacement pulses (having low frequencies) that have been associated with near-field or pulse-type ground motions [Makris 1997; Kelly 1999] in the direction of the fault-plane rupture have shown large damage-inducing ability. This is due to the large amount of energy contained in such ground motions that may be imparted to the structures through large velocity pulses [Howard et al. 2005; Zhang and Iwan 2002]. Recent simulated stationary (random) plastic analyses of single- and multi-degree of freedom buildings by [Attard and Mignolet 2005; Attard and Mignolet 2008] have verified this. The study revealed that structural damage did not exceed certain thresholds even under near-resonant conditions unless an increase in the amount of energy was supplied through the ground motion.

While the lateral force-resisting system in buildings may be significantly improved by implementing semiactive devices or various energy-dissipating devices, inherent difficulties could include time-delays and/ or the suddenness of the engaging/ disengaging behavior of these devices. [Nagarajaiah et al. 2000], and [Varadarajan and Nagarajaiah 2004] developed a semiactive device to transition smoothly thus avoiding high-frequency resonance. Variable damping devices have been developed and applied by [Symans and Reigles 2004] and [Madden et al. 2002] as part of a "hybrid" system that uses passive base isolation to avoid structural resonance and dissipate high-energy from near-field excitations. Magnetorheological (MR) fluid dampers [Gavin et al. 2003b; Gavin et al. 2003c; Gavin et al. 2003a] have been used in variable damping devices and also in combination with variable stiffness devices in smart base-isolated systems [Nagarajaiah et al. 2004; Nagarajaiah and Mao 2004] to continuously vary their stiffness and damping and remain in a low energy nonresonant state during an earthquake (through the feedback mechanism).

Control devices develop control forces using embedded control laws. Their effectiveness may be verified through benchmark testing [Ohtori et al. 2004; Reynolds and Christenson 2006] or through analytical software test beds [Caughey 1998]. Many control laws are developed assuming a linear elastic response of the structure throughout the duration of loading. However, a seismic event may cause a structure to yield and respond inelastically despite the use of a control device [Wong 2005a; Wong 2005b]. In another scenario, if the structure already contains some preexisting damage, a ground excitation, for example, may cause the damaged structural members to respond nonlinearly. Because a nonlinear response may produce a significantly different result than a linear approximation, it is important to develop a control algorithm that can accommodate the inelastic behavior of a structure [Ohtori et al. 2004]. Such control algorithms have been proposed by [Wong 2005a; Wong 2005b; Ohtori et al. 2004], and [Zhou et al. 2003]. The Predictive Optimal Linear Control (POLC) algorithm developed by [Wong 2005a; Wong 2005b] was later expanded to include inelastic structural responses using a force analogy method (FAM). This algorithm developed by Wong reduces the time delay associated with the controller unit by calculating the state space transition matrix used in the control law formulation only once rather than at each time step. This is accomplished by varying the structural displacement field rather than varying the stiffness. Because time delays can greatly reduce the efficiency of the control mechanism [Yang et al. 1990], cutting the computational time is one way to improve the overall system response. The study by [Wong 2005a; Wong 2005b] investigates the effectiveness of his algorithm in the control of inelastic structures. The algorithm was tested using various magnitudes of time delay and various control gains. The results showed that the algorithm was effective in controlling the response of various

inelastic structures, but decreased in efficiency with increased time delay due to the control force being applied out of phase with the structural displacement [Agrawal and Yang 2000].

The algorithm developed by [Ohtori et al. 2004] uses the Newmark-Beta method which is altered to accommodate a nonlinear structural system. The purpose of the study was to test the efficiency of a complete control mechanism (including structure, damper, controller, sensors, etc) using a benchmark problem, not to present a competitive design. Nonetheless, this control mechanism did offer slight to moderate improvements in the calculated structural drift and moderate to substantial improvements in the calculated floor accelerations. Further investigations of control strategies were performed by [Christenson and Emmons 2005], and [Reynolds and Christenson 2006]. Both employed a clipped-optimal H_2/LQR controller. The study performed by [Christenson and Emmons 2005] was an analytical investigation of the reliability of a semiactive control strategy. Results showed that the control strategy reduced the maximum damage to the structure compared to the uncontrolled system [Christenson and Emmons 2005]. The study performed by [Reynolds and Christenson 2006] was an experimental verification of an analytical benchmark problem. Experimental verification is important because it captures phenomena that analytical methods may not, such as higher mode effects, sensor noise, and interaction between the structure and damping device [Reynolds and Christenson 2006]. The results indicated that the control mechanism was able to control structural damage and accelerations for moderate ground motions with small amounts of nonlinear behavior but was limited when subjected to severe earthquakes that caused the structure to exhibit more significant nonlinear behavior.

The fuzzy control algorithm developed by [Zhou et al. 2003] for the control of inelastic buildings used an adaptation law to increase the robustness of the control device. The adaptation law was used to change the parameters, specifically for an MR damper. By controlling the stiffness and damping through the MR damper, the control device was able to vary its resistive force in real time to meet the current demands of the system. This enabled the control device to be effectively incorporated into buildings without prior knowledge of the building-damper interaction or the excitation it may encounter [Zhou et al. 2003].

In terms of reducing structural accelerations, the study performed by [Wong 2005a; Wong 2005b], which employed a similar control strategy (POLC expanded for inelastic structures with FAM), the acceleration response from the controlled system was higher than the response from the uncontrolled system. Investigations of active variable stiffness systems performed by [Yang et al. 1996] showed that while these types of systems are effective in minimizing interstory drifts, they may cause a significant increase in floor accelerations [Ribakov 2004].

The investigation performed herein uses the Predictive Optimal Linear Control algorithm for inelastic structures, but employs an evolutionary approach for calculating the gain in order to make the control device adaptive to the needs of the structural system in real time by meeting performance objectives at each time step. Convergence to the optimal gain value is achieved by satisfying performance objectives, which are predefined either by assuming a maximum allowable inelastic deflection, or by a maximum inelastic strain after yielding has occurred in a member, which is related to the amount of strain-energy being dissipated. The latter is more conscientious of the amount of damage that a structure may incur and also adapts to the inelasticity of the structure which is assumed to kinematically strain-harden in order to model the anisotropy experienced by the material during cyclic unloading/ reloading. The investigation formulates an optimal linear control law using an evolutionary state-transition to meet various performance objectives at each time step in both elastic- and inelastic-responding structures.

Two control algorithms are developed in this study: The first is predicated on the absolute responses of the structure, and the second uses the changes in the responses per time step ("delta responses"). It is determined that the optimal control law solution used to reduce structural damages in terms of displacements, strain energy dissipation, and acceleration reduction needs to be formulated using the delta responses using strain-based performance objectives. The procedure is entirely automated in a program developed herein, CONON (for control nonlinear time-history analysis), which simulates the optimally controlled responses of earthquake-excited systems through a feedback mechanism and evolutionary gain.

2. Analysis of damaged systems

It is believed that the time-history responses of a controlled structure needs to be calculated using a controls solution that is capable of analyzing systems that may have already yielded or have been damaged. There are three justifications for developing an inelastic evolutionary control solution. The first reason is that if a structure contains preexisting damage, then an elastic-based controls solution may not provide accurate controllability during a subsequent external excitation because the structure had already been damaged (and become inelastic), and in doing so, had lost some of its original strain energy. Secondly, even if the structure shows no signs of exterior damage, not only may some internal damage exist, but a strong unexpected earthquake may excite the structure enough to cause it to respond inelastically (beyond its elastic yield limit) during loading. Thirdly, because there are physical limitations to using external damping mechanisms, inevitable time delays due to (a) gathering sensor information/ noise interferences, (b) control device reaction time, and (c) computational delays may significantly delay when a control force is applied and preclude the structure from responding quickly enough to behave elastically and thus resulting in damage. Further, it is shown that by forcing a system to yield by continuing to apply a control force even after a performance objective has been met during unloading enables the system to dissipate some energy input to the system via the control device or by the earthquake. This is shown herein to reduce large accelerations that would otherwise occur in the structure.

The formulated controls solution generates and applies control forces on an as-needed basis during an earthquake, as opposed to applying a force at each time step [Kim and Adeli 2004; Wong and Yang 2002]. Further, the gain formulation used in the proposed solution is optimally computed at each time step as opposed to using a single gain that is only calculated initially [Franklin et al. 2002]. Also, the performance objectives are defined as allowable inelastic demands – i.e., some acceptable level of damage is permitted. In this light, control solutions based on performance objectives defined using allowable post-yield displacements are compared to those based on allowable post-elastic strains. The latter, *strain-based*, approach assumes an evolving window of acceptable inelastic strains depending on the structure's yield displacement during *each* cycle. Thus, the performance objective may be thought of as an allowable *moving* range of post-yield strains for each cycle of response.

By analyzing the control of inelastic systems, the control force may be larger than that used to control an elastic system since the damaged material would at this point provide inherently less resistance due to its already-damaged state and subsequent reduced stiffness. The large control force may result in large accelerations, which, as noted above, may then be controlled by forcing the system to yield after

unloading. In other words, additional control force may help the structure rehabilitate itself through its material hysteresis.

Controlling inelastic responses computationally prepares a controller for any potential damage that may occur. By prescribing a moving performance *window* in terms of allowable inelastic strains past yield (i.e., an allowable *range* of inelastic performances), then the control force may be significantly reduced, thus making the control device more cost-effective. The inelastic behavior itself may be defined according to the anisotropic nature of materials once they have been damaged, thus resulting in a kinematic strain hardening of the material [Wu 2005]. Therefore, the structure may experience large, yet *safe*, lateral deflections and more importantly safe inelastic strains during each cycle.

Displacement-based versus strain-based performance windows. The displacement-based performance-window is defined globally where the range of allowable lateral displacements in each member is fixed for each cycle and is measured with respect to the equilibrium position of the member (e.g., at the origin in Figure 1).

However, the inelastic strains (defined here as the post-elastic strain after yielding has occurred in a member on a given cycle) may fluctuate from cycle to cycle. Therefore, the strain-based performance window uses a moving range of inelastic strains per cycle whenever control is used, and in this sense, it may be defined as a local objective. This creates a flexible algorithm for controlling inelastic strains that controls the amount of strain energy that is dissipated, which subsequently helps to reduce the amount of permanent member damage.

In the strain-based control approach, the allowable inelastic strains are defined *per cycle* after a member has yielded. In Figure 1, the material is shown to kinematically strain harden with yield strain $1.0 \times \varepsilon_{\text{yield}}$, which corresponds to a positive (right-side) lateral deflection of 1 in; the allowable performance objective is $0.5\varepsilon_{\text{yield}}$ per cycle once the member has yielded; thus, the allowable right-side deflection is 1.5 in, and the allowable lateral deflection left of the origin is 0.5 in. This is illustrated by the solid line after yielding has occurred. In displacement-based control, however, the allowable lateral (global) deflection remains

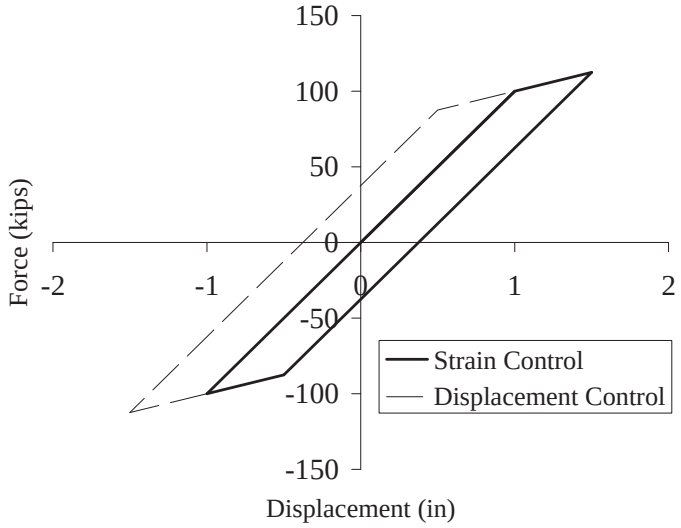

Figure 1. Illustration showing displacement control using a fixed performance window and strain control using a changing performance window.

fixed for any cycle and is independent of the hysteresis. In the Figure 1 example, the fixed global range (displacement control) is $+/-1.5$ in (shown by the dotted lines). Ultimately, the strain-based approach enables a member to dissipate less energy per cycle, and, as it will be shown later, is a better strategy for controlling inelastic damage. Further, the strain-based methodology utilizes a kinematical strain hardening approach instead of an isotropic approach, where the former models the material anisotropy in damaged systems more accurately.

Displacement-based control. A displacement-based performance objective is described as a predefined allowable displacement measured from a member's equilibrium, or undeformed, position; see Figure 2a. The equation

$$\text{(displacement-based control)} \qquad |x| > |x_{\text{perf}}| \tag{1}$$

gives the condition for applying displacement-based control, where x_{perf} is the performance objective (i.e., allowable displacement), and x is the calculated displacement that is measured at the tip of a member that has been subjected to cyclic loading; x is measured relative to the undeformed position of the member defined at the $F = 0$ axis (lateral force to the member) in Figure 2a.

By using this fixed-window approach to control displacements, the control of inelastic strains, which are cyclic-dependent, is not addressed. In other words, inelastic strains are calculated based on each new yield position of a member (and are not measured relative to the original undeformed position of the member). For a given cycle, each yield position may be different from a previous yield position and depends on the unloading/ reloading displacement (x_{unload}) for that cycle. The inelastic strain on the i-th half-cycle is proportional to the displacements (relative to the equilibrium position) as shown by (1):

$$\varepsilon_i \propto |x_{\text{unload}}| - 2|x_{\text{yield}}| + |x_{\text{perf}}|, \tag{2}$$

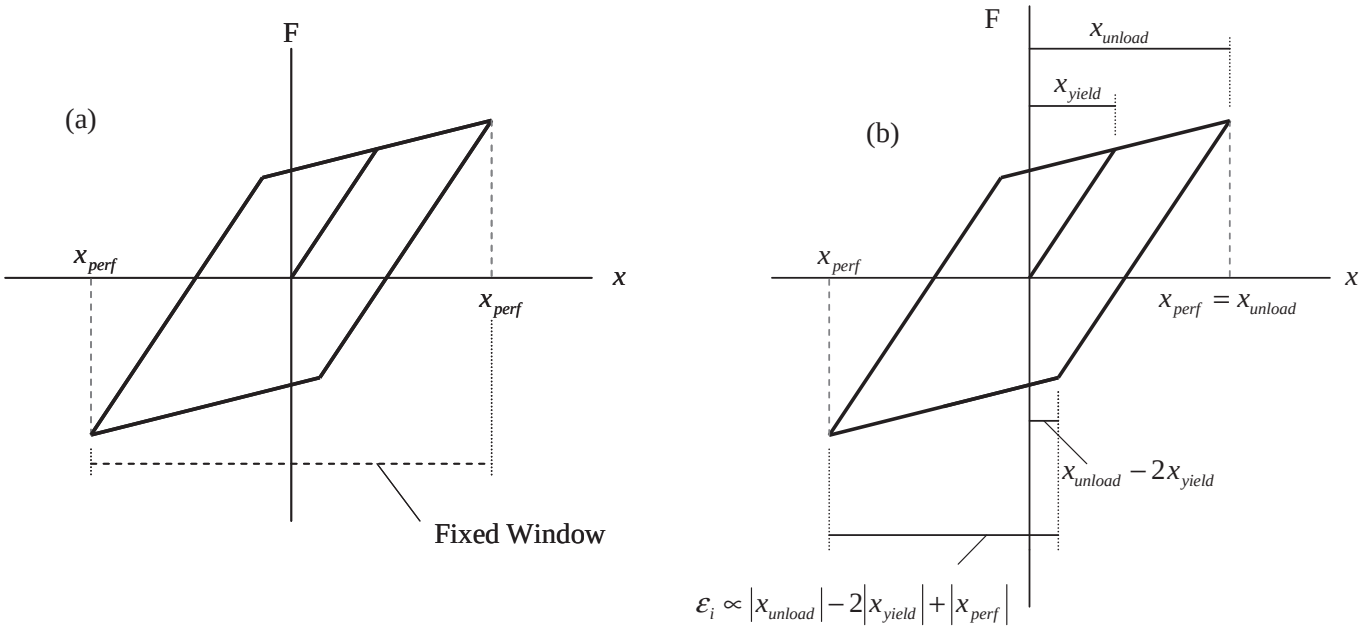

Figure 2. Displacement-based control (fixed window; left diagram) where control is called when $x = x_{\text{perf}}$ (ideal, no time-delays; right diagram).

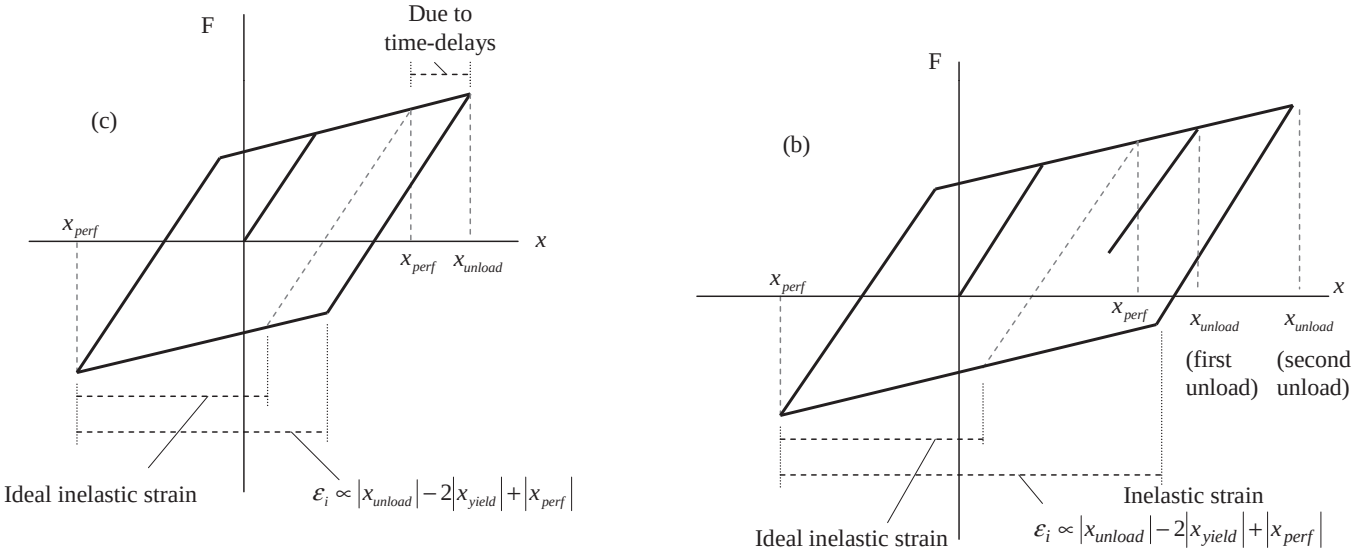

Figure 3. Displacement-based control where control is called when allowable inelastic strain is larger than the ideal inelastic strain due to (a) time delay; (b) same-side reyielding after load reversal.

where ε_i is the hysteretic half-cycle inelastic strain in the member, and x_{yield} is the displacement when a member had first yielded ($i = 1$). Figure 2b shows that $x_{\text{unload}} = x_{\text{perf}}$, which is an ideal scenario. In reality, however, sensor or controller limitations, including time-delays, result in the performance objective being exceeded before a control force is applied, where $|x| > |x_{\text{perf}}|$; see Figure 3a. Another possibility is that the control device is able to successfully unload the member ("first unload" in Figure 3b) and meet the desired performance objective, but instead of eventually yielding along this same direction, the member reverses direction and reyields at the point of first unload (the member "remembers" this most recent unload point because of the presence of residual stresses that exist in damaged members.). The control device is then required to unload the member again ("second unload" in Figure 3b). However, this second control force is significantly larger than the previous force because of the increased level of damage and accumulated strain in the member, and because of the previous injection of control force into the system. This results in an energy surplus that the member was unable to initially dissipate (by having not yielded earlier in the direction of first unload). This has several adverse repercussions, including costly control devices (requiring larger force capacity) and large acceleration demands in damaged members. Hence, load reversals may be quite harmful to a control system's capability to adequately control damaged systems; the issue is addressed later.

Strain-based control. Inelastic strain-based control enables a damaged member to dissipate less hysteretic energy than displacement-based control (Figure 1) by using a moving-window approach to satisfy performance objectives. A post-yield member displacement on each half-cycle, c, corresponds to an allowable post-yield strain measured from the point where the member yielded on that half-cycle, and not from the equilibrium position as in displacement-based control:

$$\text{(strain-based control)} \qquad \varepsilon_i \geq \varepsilon_{\text{perf}}, \quad \text{where } \varepsilon_{\text{perf}} \propto \hat{x}_{\text{perf},c}. \tag{3}$$

Here $\varepsilon_{\text{perf}}$ is the allowable strain following each yielding event and is proportional to a corresponding allowable performance displacement $\hat{x}_{\text{perf},c}$. By using such a flexible performance-window, the control algorithm may accurately converge to the desired performance objectives while remaining stable and also reducing member accelerations. Figure 4 illustrates the same scenarios as Figures 2 and 3 using strain-based control where the inelastic strain remains the same as the ideal inelastic strain. The illustrations show that strain-based control may limit the amount of inelastic strain that a member experiences, which would in turn limit the amount of strain energy that is dissipated and control member damage.

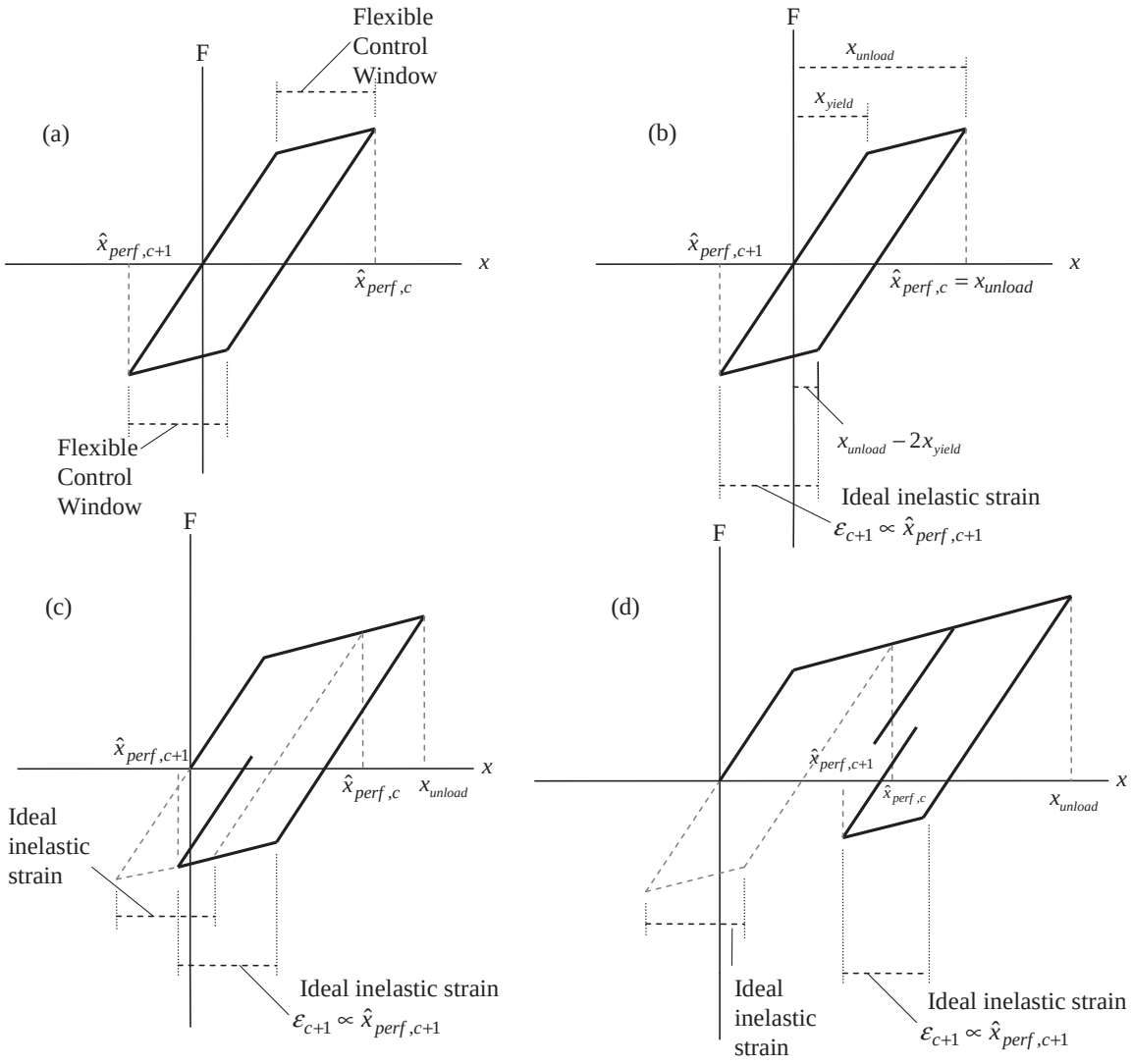

Figure 4. (a) Strain-based control (moving window) where control is called when: (b) $x = \hat{x}_{\text{perf},c}$ (allowable inelastic strain = ideal strain, no time-delays); (c) allowable inelastic strain equals the ideal inelastic strain even in the presence of time delay; and (d) allowable inelastic strain equals the ideal inelastic strain even after same-side reyielding occurs after load reversal.

Rehabilitative control: forcing members to yield. Note that in order to facilitate all further discussions, the performance objective will not be distinguished between x_{perf} (displacement-based) and $\hat{x}_{\text{perf},c}$ (strain-based); instead, x_{perf} will be commonly used. When a performance objective is exceeded (displacement x_{k+1} in Figure 5a), the "control_unload" routine is called in CONON to attempt to unload the member on the subsequent time step. If the algorithm is unsuccessful in unloading the member (possibly because of the control-induced energy that had already been residing in the system), then the algorithm proceeds to the next time step and calculates a new control force to again attempt to unload the member. This enables the material to dissipate any residual (control) energy that may have been present, thus making the member more receptive to the new imposed control. Figure 5a illustrates the application of an unloading

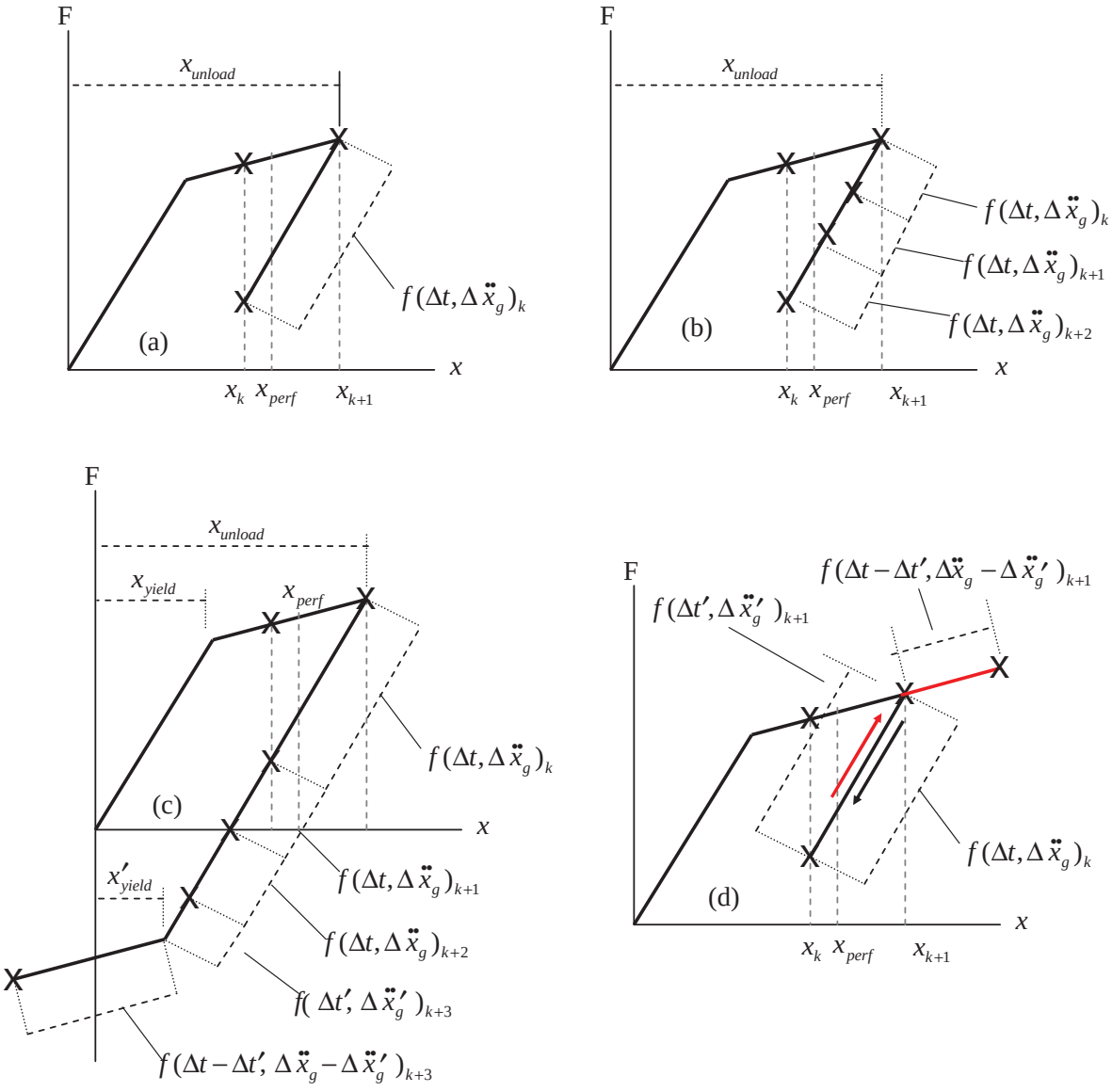

Figure 5. Controlled unloading of a member: (a) meeting the performance objective in a single time step after the member is unloaded; (b) meeting the performance objective in multiple time steps; (c) rehabilitating a member by forcing it to yield; (d) same-side reyielding after the performance objective has been satisfied.

control force over time step, Δt; the control algorithm will deactivate at the end of Δt if the performance objective is satisfied. However, if the member unloads but does not satisfy the performance objective on step k, then a new control force is calculated that is applied on the ensuing time step $(k+1)$ until the objective is finally satisfied, for example on time step $(k+2)$ as in Figure 5b.

As discussed in the preceding subsection (page 860), there are times when a performance objective may be satisfied, yet the control algorithm commands additional force to be supplied to continue unloading the member until it yields; see Figure 5c (time step $k+3$). The reason for this is to prevent same-side reyielding that would have otherwise induced additional strain hardening in the member; same-side reyielding is defined as a reversal in the member displacement and subsequent reyielding on the same-side that had originally unloaded; see Figure 5d. Thus, the forced yielding rehabilitates the structure by allowing it to dissipate any surplus energy it may have absorbed earlier. This helps reduce the velocity and acceleration of the member and maintains a stable system [Attard et al. 2009]. The time step over which the member is being forced to yield is iterated (see Figure 5c, time step $k+3$) until the necessary state-space transition matrix, $\boldsymbol{S}_s$, and control force help the member yield. A new control force is then applied over the remainder of the time step $(\Delta t - \Delta t')$ using the appropriate reduction in the member stiffness.

3. Optimal inelastic control for already-damaged structures

The control law herein is used to formulate an optimal, evolutionary gain and subsequent control force for the purpose of reducing demands that may have exceeded prescribed performance objectives. The solution is formulated in state-space. The energy-based cost function is minimized, and structural demands may be controlled *per time step*. In this sense, the control device responds to each response in real-time and employs a new gain formulation at each time step only *as-needed* for the purpose of generating an appropriate counteracting force. This approach may be used in lieu of a constant or predetermined gain formulation that is otherwise used throughout the response time history in calculating a continual resistive control force. However, when a control device adds energy (either from an evolutionary gain or a constant gain basis) into a damaged (inelastic) member, there needs to be a mechanism in place to dissipate this additional energy since the damaged member has less resistance (i.e., less of its original strain energy). Without such a mechanism, the control force may even be counterproductive and result in increased damage and instability in the member response.

The algorithm in CONON is developed using an optimal linear centralized approach that is based on linear quadratic theory [Franklin et al. 2002]. The evolutionary gain is calculated by adapting the Riccati matrix per time step, where the damaged member may either be rehabilitated (see above), or where smaller quantities of control energy are formulated and utilized per time step in the calculation of the control force (discussed later). An allowable response window is used to represent the amount of tolerable material damage in a structural member. The allowable window may remain either fixed (displacement-based control) or flexible (strain-based control), where the latter accounts for the material anisotropy in damaged members caused by the realignment of the material's molecular structure.

The equation of motion for an multi-DOF shear-frame excited by horizontal base ground accelerations, $\ddot{\boldsymbol{x}}_g(t)$, is given by

$$M\ddot{x}(t) + C\dot{x}(t) + Kx(t) = -M\ddot{x}_g(t) - F_R(t) + Df_c(t). \tag{4}$$

The location vector of the control devices having control force $f_c(t)$ is given as $\boldsymbol{D}$. The mass and damping matrices are defined as $\boldsymbol{M}$ and $\boldsymbol{C}$, respectively. The displacement vector relative to the ground is defined as $\boldsymbol{x}(t)$. The elastic stiffness is defined as $\boldsymbol{K}$, which is a linear nonhysteretic spring that provides the only restoring force to the frame until yielding occurs in the j-th member at which point the nonhysteretic spring force remains constant, and $x_j(t) = x_{\text{yield},j}$, where $x_j(t)$ is a component of $\boldsymbol{x}(t)$. The hysteretic restoring force, $\boldsymbol{F}_R$, which includes the post-yield deflection, appears in those members that have started to yield (i.e., $x_j(t) > x_{\text{yield},j}$).

$$F_R(t) = \sum_{i=1}^{\text{plex}} \alpha_{ij} K x_{ie,ij}(t), \tag{5}$$

where the proportionality factor, α_{ij}, in (5) is the ratio of the inelastic stiffness to the elastic stiffness of the j-th member in the shear-frame. The term *plex* is the number of plastic excursions that the j-th member may ultimately experience during a given half-hysteretic cycle, where i represents the state of damage in the j-th member. The separation of the elastic and inelastic stiffness components in (4) facilitates the proposed inelastic control. The inelastic displacements, $x_{ie,ij}$, in (5) may be expressed as

$$x_{ie,ij}(t) = \begin{cases} x_{\text{tot},j}(t) - x_{\text{yield},j} - \sum_{m=1}^{i-1} x_{ie,mj}(t) & \text{if } i \geq 2, \\ x_{\text{tot},j}(t) - x_{\text{yield},j} & \text{if } i = 1. \end{cases} \tag{6}$$

The displacement $x_{\text{tot},j}(t)$ is calculated relative to when the now-yielded member started to unload or reload on any given half-cycle. The degradation of the stiffness is developed by introducing a nonlinear kinematic strain hardening in the material, where on a given half-cycle, a member will reyield at a displacement equal to the most recent unloading displacement minus twice the initial yield displacement [Ragab and Bayoumi 1999]. This permits each hysteresis loop to close and merge with each preceding loop [Lemaitre and Chaboche 1990]. Additionally, the same set of α_{ij} factors are used in calculating the degraded member stiffness starting with each half-cycle. Finally, the most recent member stiffness immediately before unloading is "remembered" to account for any residual stresses in the event that a load reversal occurs and the member reyields.

Damaged (inelastic) members have less restoring force capability than undamaged (elastic) members, thus requiring larger control forces that result in high manufacturing costs. In order to minimize the requisite control force, an optimal Riccati matrix and a new (or evolutionary) gain are used during *each* necessary time step to produce an optimal control force that will help satisfy elastic or inelastic performance objectives. The procedure is entirely automated in CONON. The control force is calculated using an optimal linear closed-loop control algorithm which relies on the velocity and displacement of the structure. The control law may be expressed as

$$f_c(t) = f_{c1}(x(t)) + f_{c2}(\dot{x}(t)), \tag{7}$$

where $f_c(t)$ is the applied control force, and f_{c1} and f_{c2} are functions that govern the participation of the structure's displacement and velocity in the calculation of the control force. The objective is to determine the forms of f_{c1} and f_{c2} that will produce a control force to satisfy the desired performance objectives. Therefore, the cost function J_k in (8) is minimized subject to the constraint of the state-space response,

z_{k+1}, where

$$J_k = \int_{t_k}^{t_k+\Delta t} \tfrac{1}{2}\left(z_k^T(t)\,\boldsymbol{Q} z_k(t) + f_{c,k}^T(t)\boldsymbol{R} f_{c,k}(t)\right) dt. \tag{8}$$

The Riccati matrix is determined iteratively and is used to relate the current state-space response of the member, z_k, to a Lagrange multiplier, where the latter is used to find an expression for z_{k+1} in terms of z_k and which also leads to the calculation of the control law of $f_{c,k}$ (where k is the time step over which the control force is calculated). The cost function, J_k, is minimized per k-th time step over the time step interval, Δt, and $\boldsymbol{Q}$ and $\boldsymbol{R}$ are weighing matrices that affect the controlled responses and applied control force, respectively. The state-space response vector (for DOF degrees of freedom) is expressed as

$$z(t) = \begin{Bmatrix} x(t) \\ \dot{x}(t) \end{Bmatrix}_{(2\,\mathrm{DOF})\times 1} \tag{9}$$

and after multiplying through with $\boldsymbol{M}^{-1}$, we may express (4) in state-space form as

$$\dot{z}(t) = \boldsymbol{A} z(t) + \boldsymbol{H}\ddot{x}_g(t) + \sum_{i=1}^{\mathrm{plex}} \boldsymbol{F}_{c,ie} x_{ie,ij}(t) + \boldsymbol{B} f_c(t), \tag{10}$$

where we have introduced the following matrices:

$$\boldsymbol{A} = \begin{bmatrix} \boldsymbol{0} & \boldsymbol{I} \\ -\boldsymbol{M}^{-1}\boldsymbol{K} & -\boldsymbol{M}^{-1}\boldsymbol{C} \end{bmatrix}_{(2\,\mathrm{DOF})\times(2\,\mathrm{DOF})} \qquad \boldsymbol{H} = \begin{Bmatrix} \boldsymbol{0} \\ -\boldsymbol{I} \end{Bmatrix}_{(2\,\mathrm{DOF})\times 1} \tag{11}$$

$$\boldsymbol{F}_{c,ie} = \begin{Bmatrix} \boldsymbol{0} \\ -\alpha_{ij}\boldsymbol{M}^{-1}\boldsymbol{K} \end{Bmatrix}_{(2\,\mathrm{DOF})\times 1} \qquad \boldsymbol{B} = \begin{Bmatrix} \boldsymbol{0} \\ \boldsymbol{M}^{-1}\boldsymbol{D} \end{Bmatrix}_{(2\,\mathrm{DOF})\times 1} \tag{12}$$

Here $\boldsymbol{I}$ is the identity matrix, $\boldsymbol{0}$ is a zero vector, $\boldsymbol{H}$ is a location vector of the excited DOFs under action of the ground accelerations, $\boldsymbol{B}$ is the location vector of the control forces, and $\boldsymbol{F}_{c,ie}$ characterizes the inelastic state of the members using α_{ij}. The minimization of the cost function in (8) is a recursive procedure that may be made on any necessary time step over which a performance objective has been exceeded, thus leading to the calculation of the state-space response z_{k+1} on time step $k+1$:

$$z_{k+1} = \boldsymbol{S}_{s,k+1} z_k + \boldsymbol{G}\boldsymbol{B}^{-1}\boldsymbol{H}\ddot{x}_{g,k}(t) + \boldsymbol{G}\boldsymbol{B}^{-1}\sum_{i=1}^{\mathrm{plex}} F_{c,ie} x_{ie,i}(t), \tag{13}$$

where

$$\boldsymbol{G} = \boldsymbol{A}^{-1}(e^{\boldsymbol{A}\Delta t} - \boldsymbol{I})\boldsymbol{B} \tag{14}$$

and

$$\boldsymbol{S}_{s,k+1} = I e^{\boldsymbol{A}\Delta t} + \boldsymbol{G}[\Gamma_{k+1}^{\mathrm{ev}}]. \tag{15}$$

The evolution of the state-space transition matrix, $\boldsymbol{S}_s$, is a function of the gain (expressed by $\Gamma_{k+1}^{\mathrm{ev}}$, the evolutionary gain matrix), and transitions the response from time step k to step $k+1$, while enabling z_{k+1} to converge to the predefined performance objective z_{perf}. The evolutionary gain matrix, $\Gamma_{k+1}^{\mathrm{ev}}$, is a function of the Riccati matrix, $\boldsymbol{P}_{k+1}$, which is calculated iteratively so that $\boldsymbol{P}_{k+1} \sim \boldsymbol{P}_k$:

$$\boldsymbol{P}_{k+1} = \boldsymbol{Q} + (e^{\boldsymbol{A}\Delta t})^T \boldsymbol{P}_k (I + \boldsymbol{G}\boldsymbol{R}^{-1}\boldsymbol{G}^T\boldsymbol{P}_k)^{-1} e^{\boldsymbol{A}\Delta t}. \tag{16}$$

The evolutionary gain may be expressed as

$$\Gamma_{k+1}^{\text{ev}} = -(\boldsymbol{G}^T \boldsymbol{P}_{k+1} \boldsymbol{G} + \boldsymbol{R})^{-1} \boldsymbol{G}^T \boldsymbol{P}_{k+1} e^{\boldsymbol{A}\,\Delta t} \tag{17}$$

and the control force as

$$f_{c,k+1} = [\Gamma_{k+1}^{\text{ev}}] z_k. \tag{18}$$

The minimization of the total state-space response, $z(t)$, over the entire time history may finally be expressed as

$$J = \sum_{k=1}^{\text{TimeCount}} \int_{t_k}^{t_k+\Delta t} \tfrac{1}{2} \left(z_k^T(t)\, \boldsymbol{Q} z_k^T(t) + f_{c,k}^T(t) \boldsymbol{R} f_{c.k}^T(t) \right) dt, \tag{19}$$

where TimeCount is the number of time steps in CONON's numerical simulation algorithm.

4. Control force methodology: absolute-Z approach versus delta-Z approach

Two methods are used to calculate an optimal control force, $f_{c,k+1}$. In the first, the gain is used in conjunction with the absolute displacement of the structure while the second approach employs the gain in conjunction with the absolute value of the difference between the exceeded displacement (x_{k+1}) and x_{perf}, where x_{perf} and $\dot{x}_{\text{perf}}$ are the performance objectives for displacement and velocity, respectively. The former approach is referred to herein as the absolute-Z approach, and we will refer to the latter as the *delta-Z approach*. The absolute-Z approach uses the state-space response in (9) to minimize the cost function in (19) over the time history. In the delta-Z approach, Equations (8) and (9) are modified to include difference (or "delta") components, Δz_k, on each time step:

$$J_k = \int_{t_k}^{t_k+\Delta t} \tfrac{1}{2} \left(\Delta z_k^T(t) Q \Delta z_k(t) + f_{c,k}^T(t) R f_{c,k}(t) \right) dt, \tag{20}$$

where

$$\Delta z_k = \begin{Bmatrix} |x_k - x_{\text{perf}}| \\ |\dot{x}_k - \dot{x}_{\text{perf}}| \end{Bmatrix}. \tag{21}$$

It is assumed that $\dot{x}_{\text{perf}}$ is zero after applying the control force

$$f_{c,k+1} = [\Gamma_{k+1}^{\text{ev}}] \Delta z_k. \tag{22}$$

If, after calculating $f_{c,k+1}$ and solving for z_{k+1} in (13) via the minimization of (8), it is found that $x_{k+1} \neq x_{\text{perf}}$, then a new control force $f_{c,k+1,n}$ is calculated on that same time step $k+1$, where n represents the iteration number on time step $k+1$. The iteration continues until the performance objective is satisfied using the same value of $\boldsymbol{P}_{k+1}$; see (16), during that time step. New $\boldsymbol{Q}_n$ and $\boldsymbol{R}_n$ values are calculated on the n-th iteration by multiplying previous $\boldsymbol{Q}_{n-1}$ and $\boldsymbol{R}_{n-1}$ by scale factors, $\beta_{x,k+1,n}$, $\beta_{\dot{x},k+1,n}$, and $\gamma_{k+1,n}$. This results in a new $\Gamma_{k+1,n}^{\text{ev}}$, which is used to calculate a new force $f_{c,k+1,n}$ in (22). The factors $\beta_{x,k+1,n}$,

$\beta_{\dot{x},k+1,n}$, and $\gamma_{k+1,n}$ are determined using the displacement $x_{k+1,n-1}$:

$$\left.\begin{aligned}\beta_{x,k+1,n} &= \frac{|x_{k+1,n-1} - x_{\text{perf}}|}{x_{\text{perf}}}\beta_{x,k+1,n-1}\\ \beta_{\dot{x},k+1,n} &= \frac{|x_{k+1,n-1} - x_{\text{perf}}|}{x_{\text{perf}}}\beta_{\dot{x},k+1,n-1}\\ \gamma_{k+1,n} &= \frac{|x_{k+1,n-1} - x_{\text{perf}}|}{x_{\text{perf}}}\gamma_{k+1,n-1}\end{aligned}\right\} \quad \text{for } n \geq 2, \tag{23}$$

where $x_{k+1,1}$ may be calculated using (13) and (9). Initially, $\boldsymbol{Q}$ and $\boldsymbol{R}$ (see [Hart and Wong 2000] and [Conner 2003]) are defined as

$$\boldsymbol{Q} = \begin{bmatrix}\boldsymbol{K} & 0\\ 0 & \boldsymbol{M}\end{bmatrix}, \qquad \boldsymbol{R} = [\boldsymbol{I}]. \tag{24}$$

The scale factors are applied over each iteration; the parameter $\beta_{x,k+1,n}$ multiples $\boldsymbol{K}$, $\beta_{\dot{x},k+1,n}$ multiplies $\boldsymbol{M}$, and $\gamma_{k+1,n}$ multiplies $\boldsymbol{R}$. The evolution of $\Gamma^{\text{ev}}_{k+1,n}$ occurs iteratively on each time step whenever the performance objective has been exceeded. This forces the damaged (inelastic) members to unload without significantly overshooting the prescribed objective – either for an allowable displacement (displacement-based control) or allowable inelastic strain (strain-based control). In addition, the velocity and acceleration demands are reduced because $\dot{x}_{\text{perf}}$ is assumed to be 0. In a "constant" gain formulation, $\boldsymbol{Q}$ and $\boldsymbol{R}$ remain constant, which may hinder the inelastic structure from unloading even after the performance objective has been exceeded. Further, a constant gain may potentially infuse a structure with too much energy and make it unstable [Attard and Dansby 2008].

There are three advantages to using the delta-Z approach over the absolute-Z approach and thereby working with smaller demands, $x_k - x_{\text{perf}}$:

(1) The control device needs to dissipate smaller quantities of energy during each time step and therefore generate smaller control forces that result in smaller device costs.

(2) The convergence algorithm in CONON for meeting the performance objectives remains consistently stable.

(3) The velocity and acceleration responses of the structure are significantly reduced.

Since the control algorithm uses a delta state response vector, Δz_k, as input — see (21) — the solution (i.e., the output) to (13) is also in "delta" form and is calculated as Δz_{k+1} in (25).

$$\Delta z_{k+1} = S_{s,k+1}(\Delta z_k) + GB^{-1}H\ddot{x}_{g,k}(t) + GB^{-1}\sum_{i=1}^{\text{plex}} F_{c,ie}x_{ie,i}(t). \tag{25}$$

To convert Δz_{k+1} to the new state response (i.e., to the new delta displacement and velocity), Δz_{k+1} is added to z_{perf}, which results in the new state response

$$z_{k+1} = \Delta z_{k+1} + z_{\text{perf}}. \tag{26}$$

The error between x_{k+1} and the performance displacement, x_{perf}, on the $(k+1)$-th time step is

$$\text{err}_{k+1} = \frac{|\Delta x_{k+1}|}{|x_{\text{perf}}|}, \tag{27}$$

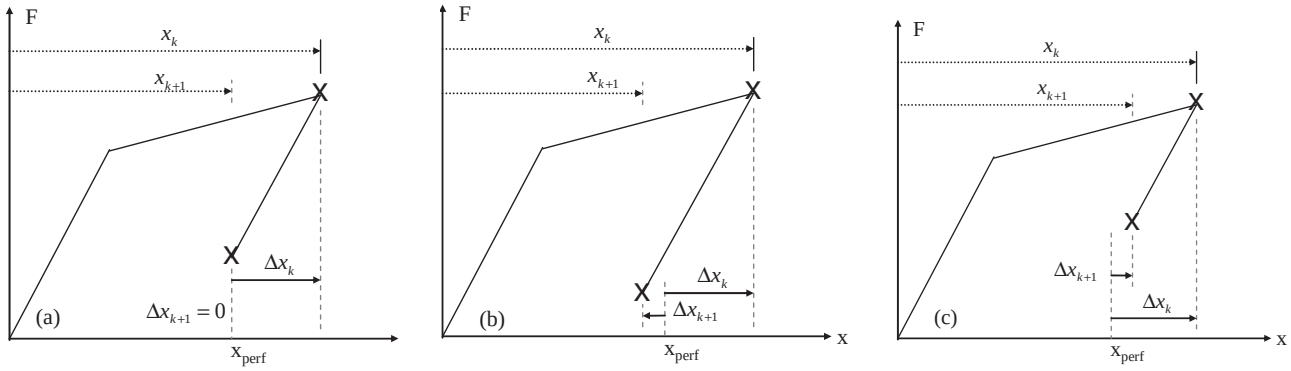

Figure 6. Illustration of the delta-Z approach: Δx_{k+1} is measured from the performance objective, or x_{perf} with (a) $\Delta x_{k+1} = 0$, where the performance objective is satisfied exactly, (b) $\Delta x_{k+1} < 0$, where the performance objective is over-shot, and (c) $\Delta x_{k+1} > 0$, where the performance objective is under met and not satisfied.

where

$$\Delta x_{k+1} = x_{k+1} - x_{\text{perf}}. \tag{28}$$

If err_{k+1} does not exceed a predefined error, the performance objective was satisfied on time step $(k+1)$; see Figure 6a. However, if $|x_{k+1}| < |x_{\text{perf}}|$, the performance objective was met and exceeded (over-shooting), and the algorithm proceeds to the next time step; see Figure 6b. $|x_{k+1}| > |x_{\text{perf}}|$, the target displacement was not met; see Figure 6c. In this last case, a control force is calculated again using (22), and the process repeats until the predefined error is not exceeded. This flowchart below illustrates the delta-z approach:

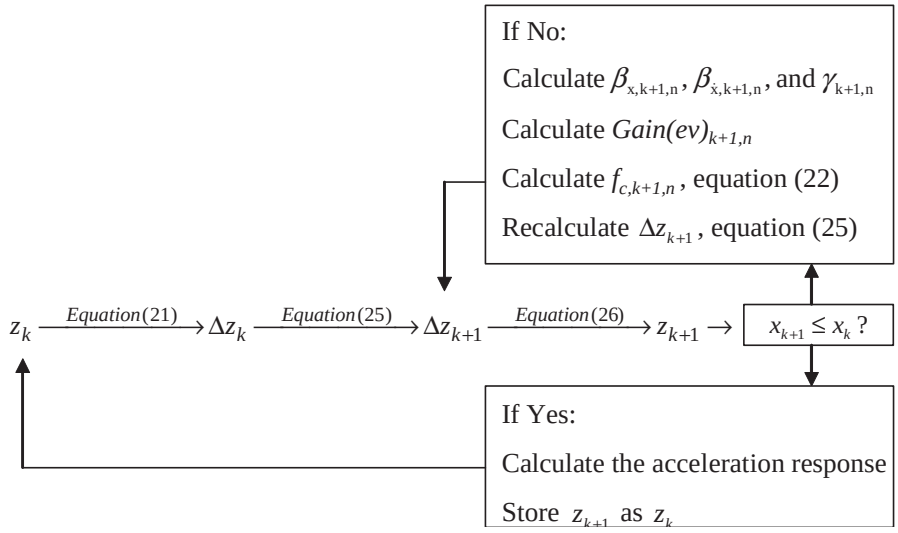

5. Numerical examples

In the following examples, CONON used the state-space formulation discussed above when it was necessary to simulate the gain evolution and control responses (i.e., when the performance–objective had been exceeded). During all other time steps (when control was not necessary), the response time histories were marched by the Newmark Beta scheme assuming a linear change in the acceleration between time

section	W12×50 (W310×74)
mass m	0.5 kips-s^2/in (87.5 kN-s^2/m)
modulus E	29000 ksi (200 GPa)
length L	12 ft (3.66 m)
σ_{yield}	36 ksi (248 MPa)

Table 1. Single-DOF properties of the benchmark system.

steps. In either case, the time steps (Δt) were separated 0.02 seconds apart until the final time of the input earthquake starting from zero initial conditions. The properties of the single-DOF benchmark system used in the following examples are shown in Table 1. The analyses assumed rock-like ground conditions and 5% damping. The benchmark structure is modeled using two 3.65 m (12 ft) columns having total elastic stiffness of 160.8 kN/cm and an elastic natural frequency of 2.15 Hz (for initially fixed-fixed connections). The structural responses were simulated using the first 20 seconds of the El Centro ground acceleration record (S00E component) of the 1940 Imperial Valley Earthquake. In the cases where the calculated displacement at the tip of each column was not permitted to exceed the yield limit (e.g., to safeguard against potential time-delays), the prescribed performance objective was calculated as a percentage (under 100%) of the yield deflection, x_{yield} (which equaled 0.705 in), and the predefined error was taken as 0.1%; see (27). When the displacement exceeded x_{yield}, the post-yield stiffness degradation in each member was calculated using $\alpha_{11} = 0.18$ [Attard 2005] in (5) and (12); and a value of 1 was used for the constant plex in (5).

The W12 × 50 sections are assumed to kinematically strain harden, which accounts for the material anisotropy when the members unload/reload as shown in the main graph of Figure 7. The elastic (ε^e)

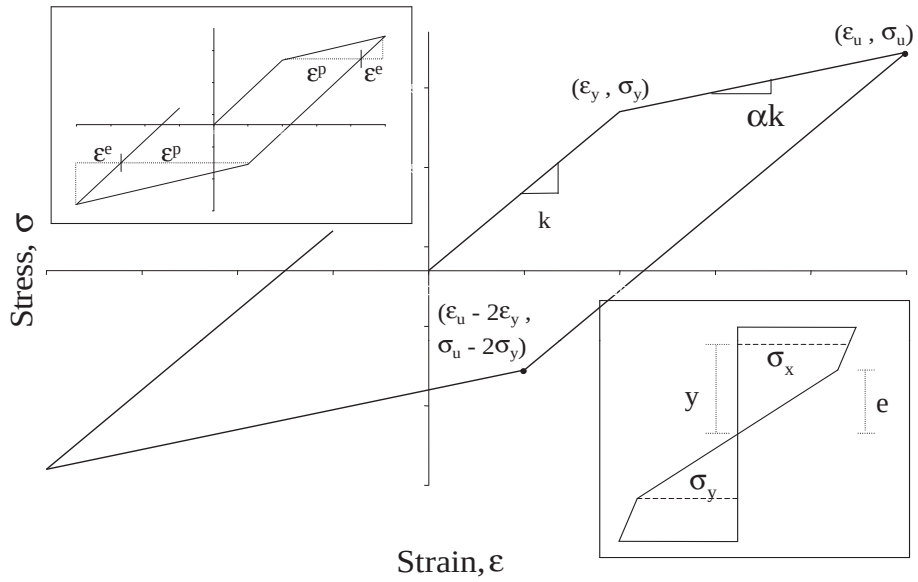

Figure 7. Model of kinematic strain hardening (anisotropic hardening). The insets show the elastic and plastic strain components (upper left) and through-thickness stress distribution (lower right).

and plastic (ε^p) strain components are shown in the inset graph on the top left, and the bilinear stress function (σ_x) used herein to calculate the post-yield stresses in the members once their cross-sections have yielded is calculated according to (29), where y is the depth to σ_x, and e is the elastic depth in the through-thickness of the cross-section; this is shown in the graph at the bottom right of the figure.

Embedding in CONON the model described by Figure 7 and the equation

$$\sigma_x = \sigma_y + \sigma_y \alpha_1 \left(\frac{y}{e} - 1 \right) \quad \text{for } y \geq e. \tag{29}$$

we obtain the benchmark responses of the single-DOF system (using no control) shown in Figure 8.

Constant gain. Two ways of applying a constant gain were investigated. First, a constant gain was applied in an always-on condition every other time step ($2x\,\Delta t$, or every 0.04 seconds) to build a conservative time delay into the response simulation. Secondly, a constant gain was applied after the performance objective had been exceeded, thus enabling control to be used in an as-needed condition.

Always-on condition. In a simulation (noted as case 1) of the single-DOF system (see Table 1) using the always-on condition, the following scale factors were determined using the absolute-Z approach

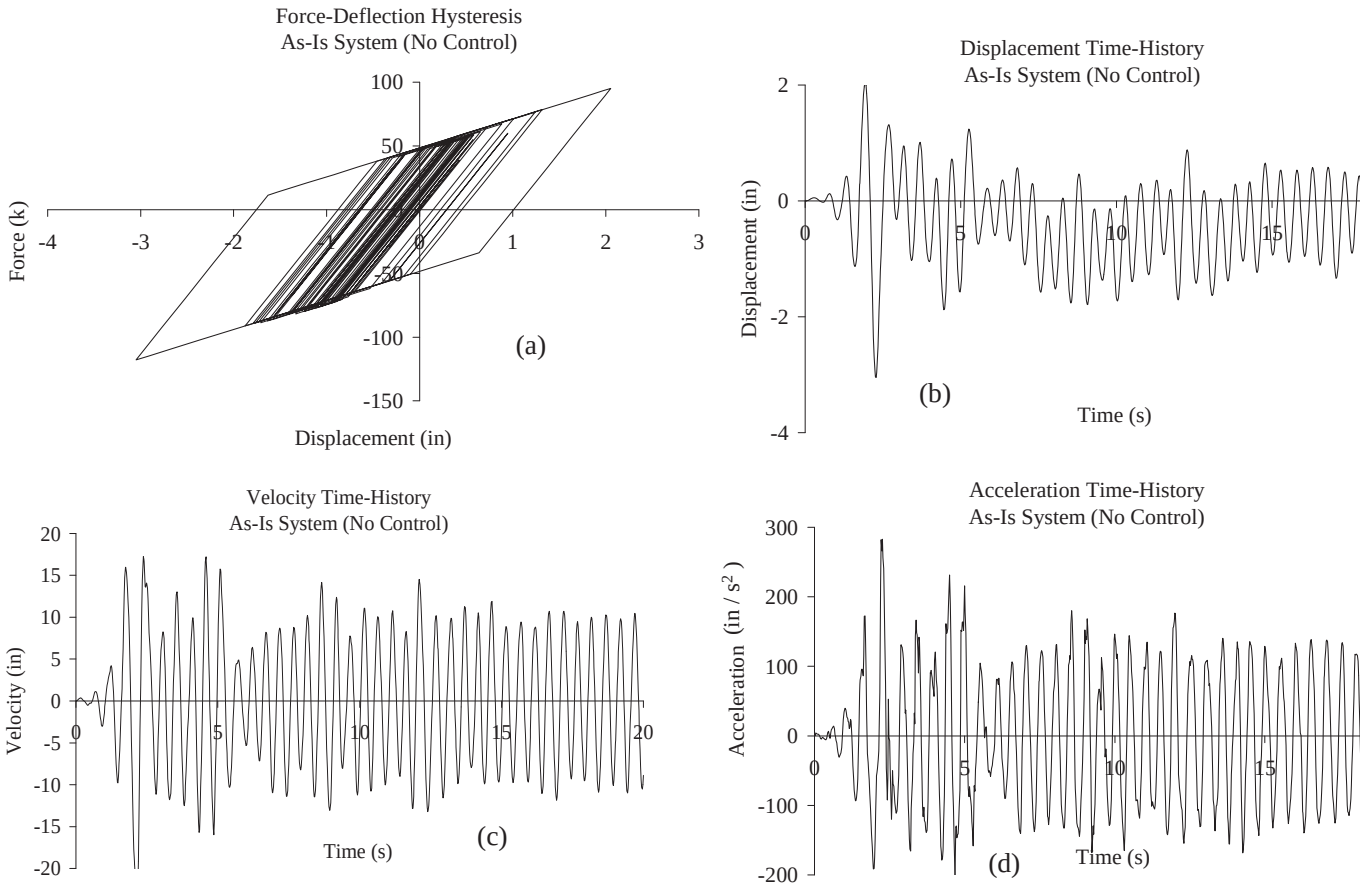

Figure 8. Benchmark shear-frame simulation (as-is system using no control): (a) force-displacement hysteresis; (b) displacement time histories; (c) velocity time histories; (d) acceleration time histories.

assuming a performance objective of 0 in measured at the tip of the column on the top story: $\beta_x = 0.32768$, $\beta_{\dot{x}} = 0.0032768$, and $\gamma = 3.2 \times 10^{-6}$. These values were calculated by minimizing J in (19) in individual time-history simulations of the El Centro earthquake, where the least square error of the demands was minimized over several simulations. The subsequently calculated optimal matrices $\boldsymbol{Q}$ and $\boldsymbol{R}$ were then used to control the single-DOF displacements, which remained elastic, during the earthquake using a constant gain in an always-on condition. The maximum calculated acceleration, 0.77 g's, was actually larger than the uncontrolled maximum acceleration, which was 0.73 g's, and the maximum control force that was required was 210 kips. By using an optimal always-on constant-gain control condition with a 0 in performance objective, the member displacements, while elastic, were not insignificant not to mention the relatively significant member accelerations that were found. The study implies the obvious limitations of using a constant gain approach to control.

In a case 2 simulation, the same parameters were used but using a delta-Z approach, where the system again responded elastically but incurred a maximum acceleration of 2.46 g's and a maximum control force of 495 kips at 2.3 seconds. The maximum displacement occurred one time step earlier at 2.28 seconds, which explains the large velocity and acceleration in response to the application of the preceding large control force. An as-needed condition was again assumed, and in this case, the system responded elastically only when the performance objective was defined not larger than 10% of yield, or 0.074 inches. This further illustrates the overall inefficiency of a constant gain formulation.

In a case 3 simulation, a more arbitrary selection of the scale factors in (23), where $\beta_x = 0.001$, $\beta_{\dot{x}} = 0.00001$, and $\gamma = 0.01$, shows the limitations of constant gain. In this case, the gain is applied in the always-on state using the absolute-Z approach. The performance objective is again defined as 0 in and is measured at the top story of the steel frame. After simulating the response for two cycles, the hysteresis showed that the control algorithm was unable to continue restraining the system, which became unstable with uncontrollable increases in the member displacements.

In a case 4 simulation, the delta-Z approach was used to calculate a maximum single-DOF acceleration of 0.49 g's and a maximum control force of only 0.8 kips although the displacements are once again not insignificant considering that a 0i performance objective was prescribed. The results (again using constant gain) for this last case are shown in Figure 9, which illustrates a significant reduction in the acceleration time histories compared to the uncontrolled system's accelerations.

Evolutionary gain. The four simulation cases above emphasize the importance of needing an alternative to a constant gain approach. The proposed evolutionary gain formulation is shown to desensitize the member responses to the weighing matrices while adequately controlling displacements (where little error is tolerated). The following six control scenarios were simulated using CONON:

1. absolute-Z approach, displacement-based, not forced to yield
2. absolute-Z approach, displacement-based, forced to yield
3. absolute-Z approach, strain-based, not forced to yield
4. absolute-Z approach, strain-based, forced to yield
5. delta-Z approach, displacement-based, not forced to yield
6. delta-Z approach, strain-based, not forced to yield

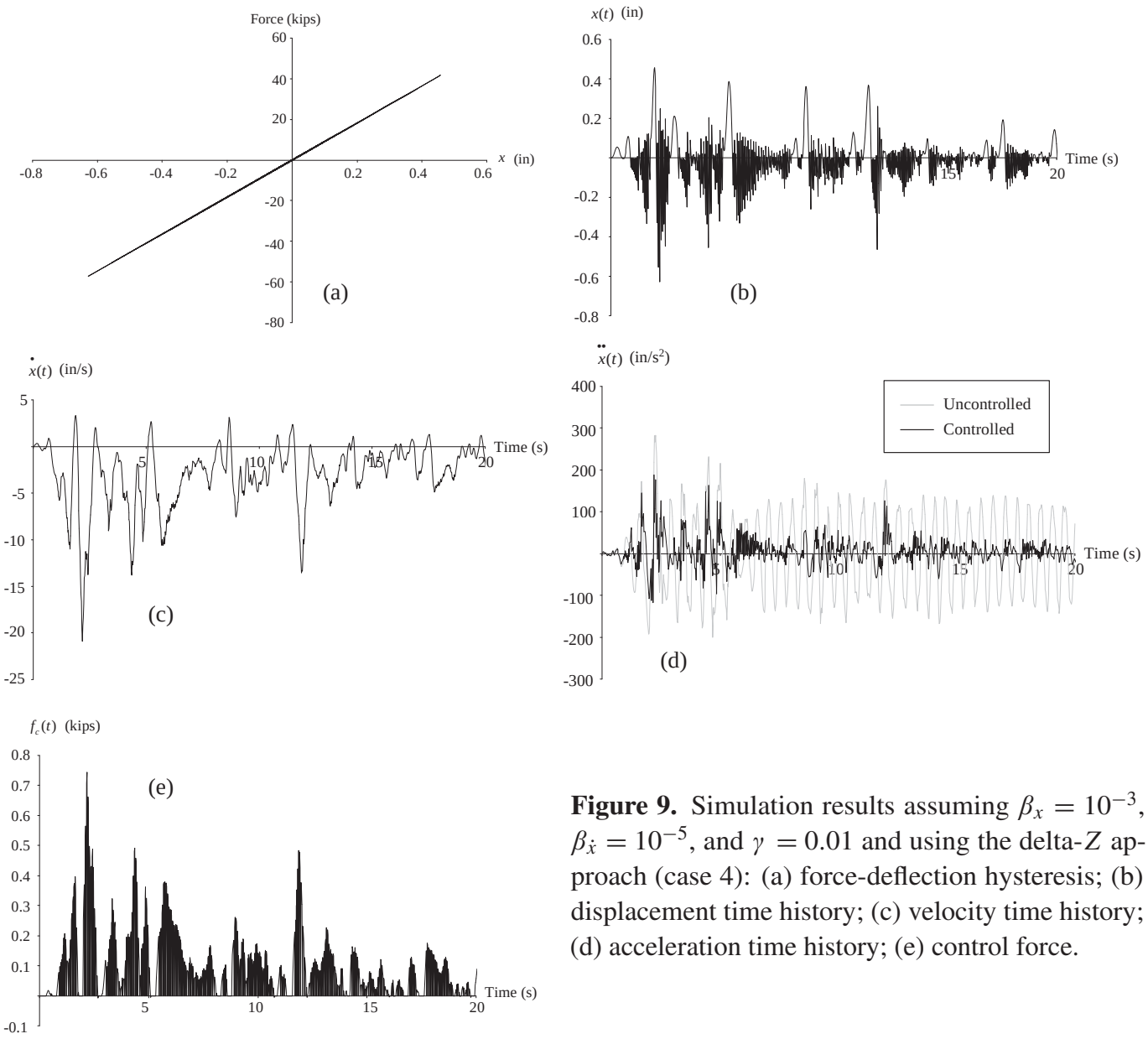

Figure 9. Simulation results assuming $\beta_x = 10^{-3}$, $\beta_{\dot{x}} = 10^{-5}$, and $\gamma = 0.01$ and using the delta-Z approach (case 4): (a) force-deflection hysteresis; (b) displacement time history; (c) velocity time history; (d) acceleration time history; (e) control force.

In each case, the gain may be varied at necessary time steps in order to satisfy the performance objectives of the single-DOF system.

In the delta-Z approach, it was found that forcing the system to yield was not necessary because of the small quantities used to calculate the control forces; see (21). As such, the responses remained easily controllable without needing to force additional energy to be dissipated through member yielding, where same-side reyielding was not an issue.

Always-on condition. An evolutionary gain was calculated every other time step depending on the current state of the system. The results are shown in Figure 10 using the absolute-Z approach.

The force-deflection hysteresis in Figure 10a shows that when control remains in an always-on state, the system responded elastically — at about 20% of the yield displacement. The controlled displacements were also significantly reduced compared to the uncontrolled displacement, as is seen from the time

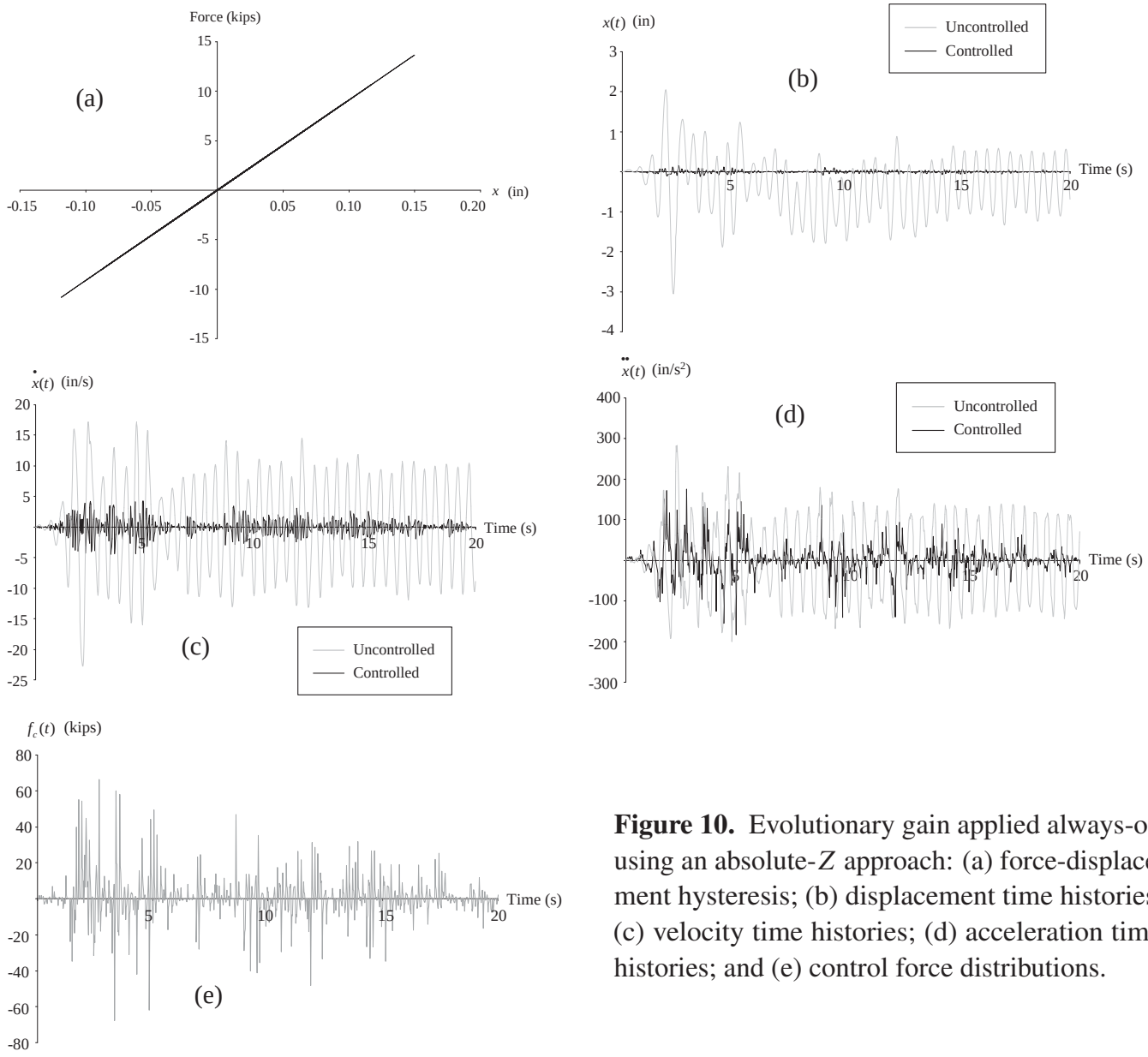

Figure 10. Evolutionary gain applied always-on using an absolute-Z approach: (a) force-displacement hysteresis; (b) displacement time histories; (c) velocity time histories; (d) acceleration time histories; and (e) control force distributions.

histories in Figure 10b. The velocity and acceleration time histories, shown in Figures 10c,d, were also smaller, and the maximum calculated control force, shown in Figure 10e, was 59 kips. If to compare these responses to those calculated in case 1 above (absolute-Z approach, always-on state) which had used a constant gain formulation, the evolutionary-controlled displacements are smaller, the accelerations are smaller (0.48 g's versus 0.77 g's), and the control force is significantly less (59 kips versus 210 kips). By varying the gain, the spikes observed in the velocity and acceleration responses of the constant gain system were alleviated since the infused earthquake energy was being dissipated from the structure in an optimal sense with respect to the exact necessary amount of gain.

The results using the delta-Z approach are virtually identical to those using the absolute-Z approach, where the responses are smaller than those of the uncontrolled system, and smaller than those using a constant gain approach (see case 2 above).

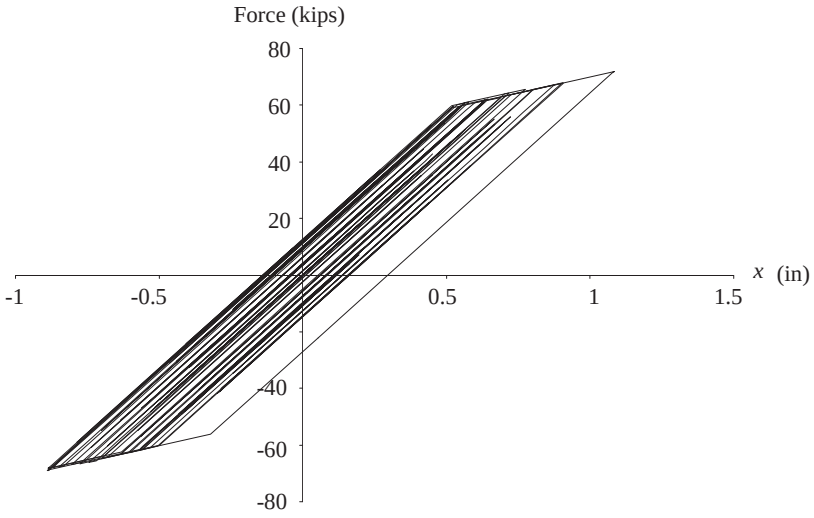

Figure 11. Force-deflection hysteresis using an evolutionary gain, and a performance objective of 50% of deflection at yield. Note that the response becomes inelastic.

As-needed condition. It was next desired to apply a control force only when needed, i.e., when the calculated displacement exceeded the allowable prescribed displacement. First, an elastic performance objective was defined - in this case, 50% of the yield deflection, or 0.352 in. The force-deflection hysteresis in Figure 11 used the absolute-Z approach and reveals that even with an elastic performance objective well below the yield deflection, the structure may still respond inelastically due to the inherent time-delay in the controller. In this case, a maximum deflection of 1.06 in was calculated, which exceeded the target displacement (50% of yield) by more than 3 times. As previously noted, the control of inelastic structures is an important consideration because of time delays, possible preexisting damages that may have altered the material constituency (e.g., the stress-strain curve), and because of unexpected earthquakes.

Next, focusing only on inelastic performance objectives, the differences between displacement-based control and strain-based control and the advantages of using the delta-Z approach over the absolute-Z approach are examined. In the strain-based control case, less energy is generally dissipated per cycle through the material hysteresis (see Figure 1), which helps preserve the structural member's resistance and prevent further damage. Table 2 lists two evolutionary gain investigations consisting of displacement-based and strain-based performance objectives for inelastic control.

performance objective	displacement-based		strain-based	
	% of first yield	allowable deflection (in)	post-yield strain	post-yield deflection (in)
Investigation 1	125	$1.25 \times 0.704 = 0.881$	$0.25\,\varepsilon_{\text{yield}}$	0.176 $(= 0.881 - 0.704)$
Investigation 2	375	$3.75 \times 0.704 = 2.642$	$2.75\,\varepsilon_{\text{yield}}$	1.937 $(= 2.642 - 0.704)$

Table 2. Performance-objective criteria for two evolutionary-gain investigations.

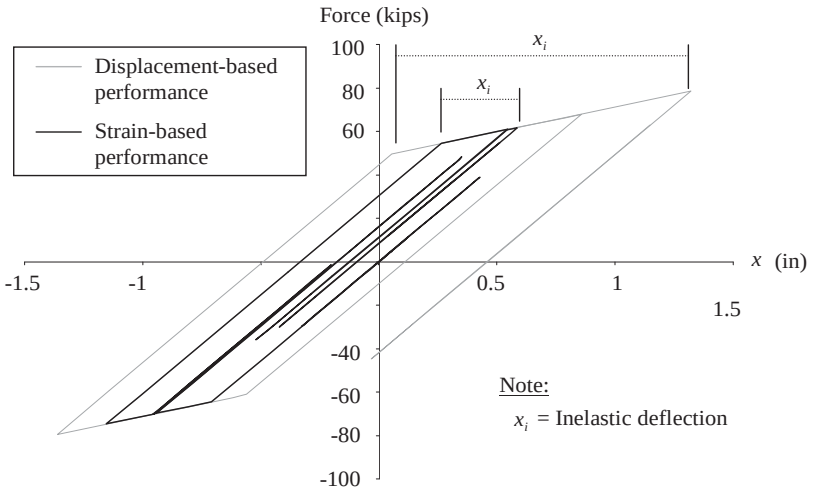

Figure 12. Hysteresis responses comparing inelastic control using displacement-based versus strain-based performance objectives.

Investigation 1. A strain-based performance objective helps minimize structural damage by controlling the amount of strain-energy that a member dissipates. The force-displacement hysteresis in this investigation is shown in Figure 12, which compares the simulated responses after 2.8 seconds using a strain-based performance objective to those of a displacement-based performance objective. The former enables the member to experience less inelastic displacement (and less strain energy dissipation) and consequently less structural damage.

Figure 13 shows the system responses using a displacement-based performance objective, without forcing the system to yield.

Referring to the force-deflection hysteresis in Figure 13a, the controlled structure's maximum deflection is less than that of the uncontrolled structure; however, if the amount of damage is a direct measure of the amount of dissipated strain energy, which is indicative of cyclic member behavior, then the controlled system dissipates nearly 3.6 times the strain energy of the uncontrolled system. Further, in this first investigation, the acceleration time histories reveal that the maximum acceleration for the controlled structure is about 10 times larger that those of the uncontrolled structure and is unacceptable.

However, by forcing the system to yield after the performance objective is met, the energy that is put into the system by the controller is reduced, and the controlled response remains stable. Figure 14a shows that when the system is forced to yield, the maximum displacement decreases, and more importantly, the strain energy dissipation reduces by 20% compared to the uncontrolled system and reduces by about 78% compared to the controlled system when it is not forced to yield. Therefore, forcing the system to yield ultimately precludes the system from reyielding on the same-side, which means that less energy is input into the system by the controller whereby the system remains stable and remains easier to control. As a result, not only is the overall damage reduced, but smaller control forces are also required (Figure 14b), since response reversals (same-side reyielding) necessitate larger control forces in order to meet performance objectives.

Figure 15 shows the system's response when using a strain-based performance objective compared against the uncontrolled responses. The force deflection hysteresis (Figure 15a) shows a significant

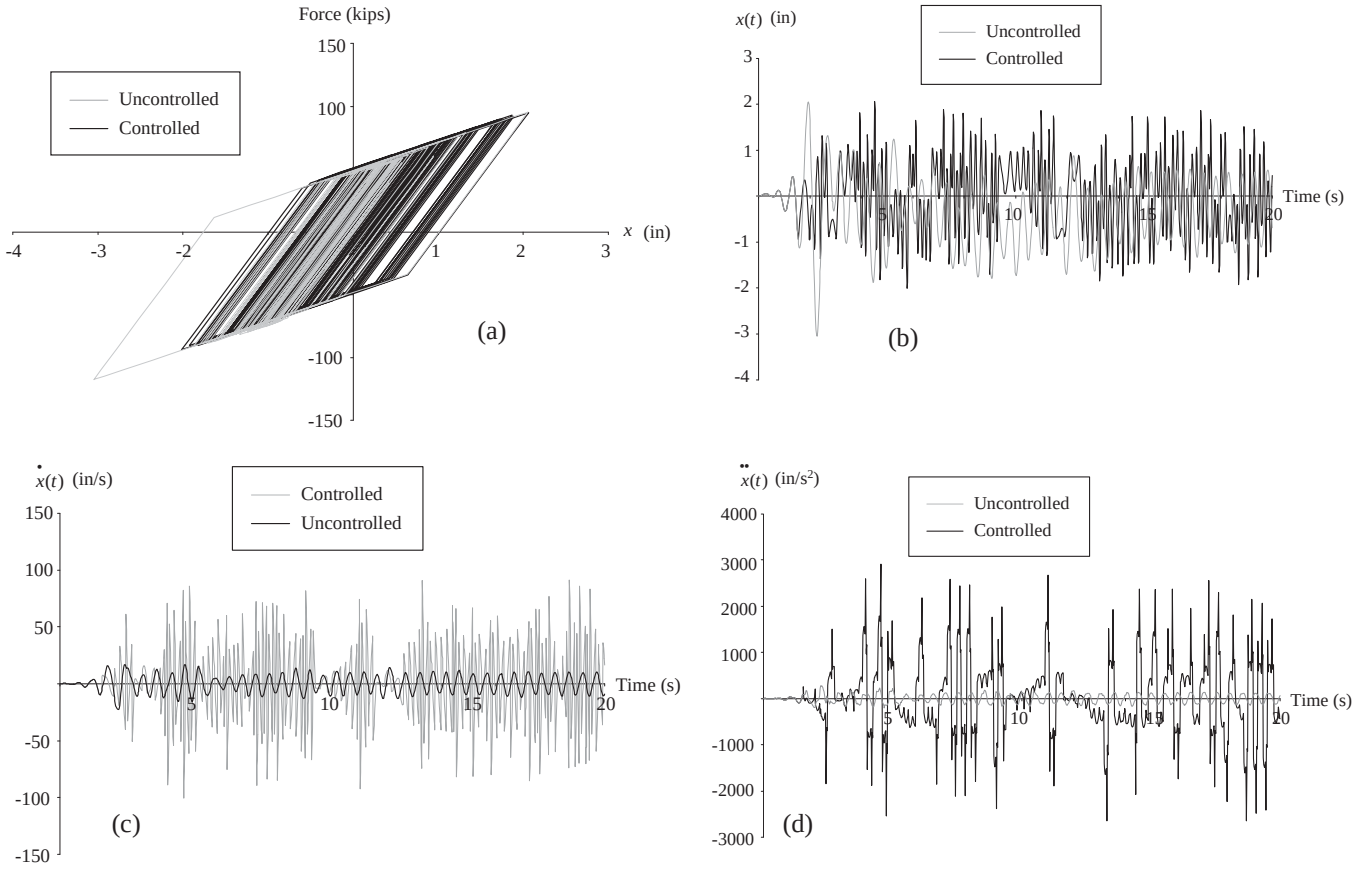

Figure 13. Responses using an evolutionary gain and the absolute-Z approach, with a displacement-based performance objective of 125% of the yield deflection (0.8805 in): (a) force-displacement hysteresis; (b) displacement time history; (c) velocity time history; and (d) acceleration time history.

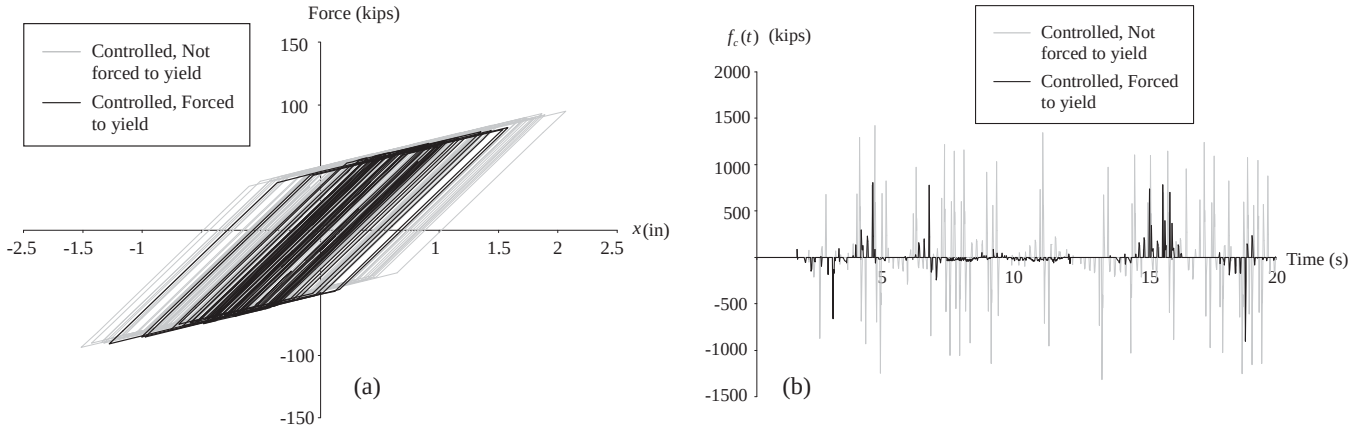

Figure 14. Evolutionary gain and the absolute-Z method, with a displacement-based performance objective of 125% of the yield deflection and forcing the system to yield: (a) force-deflection curve; (b) control force time history.

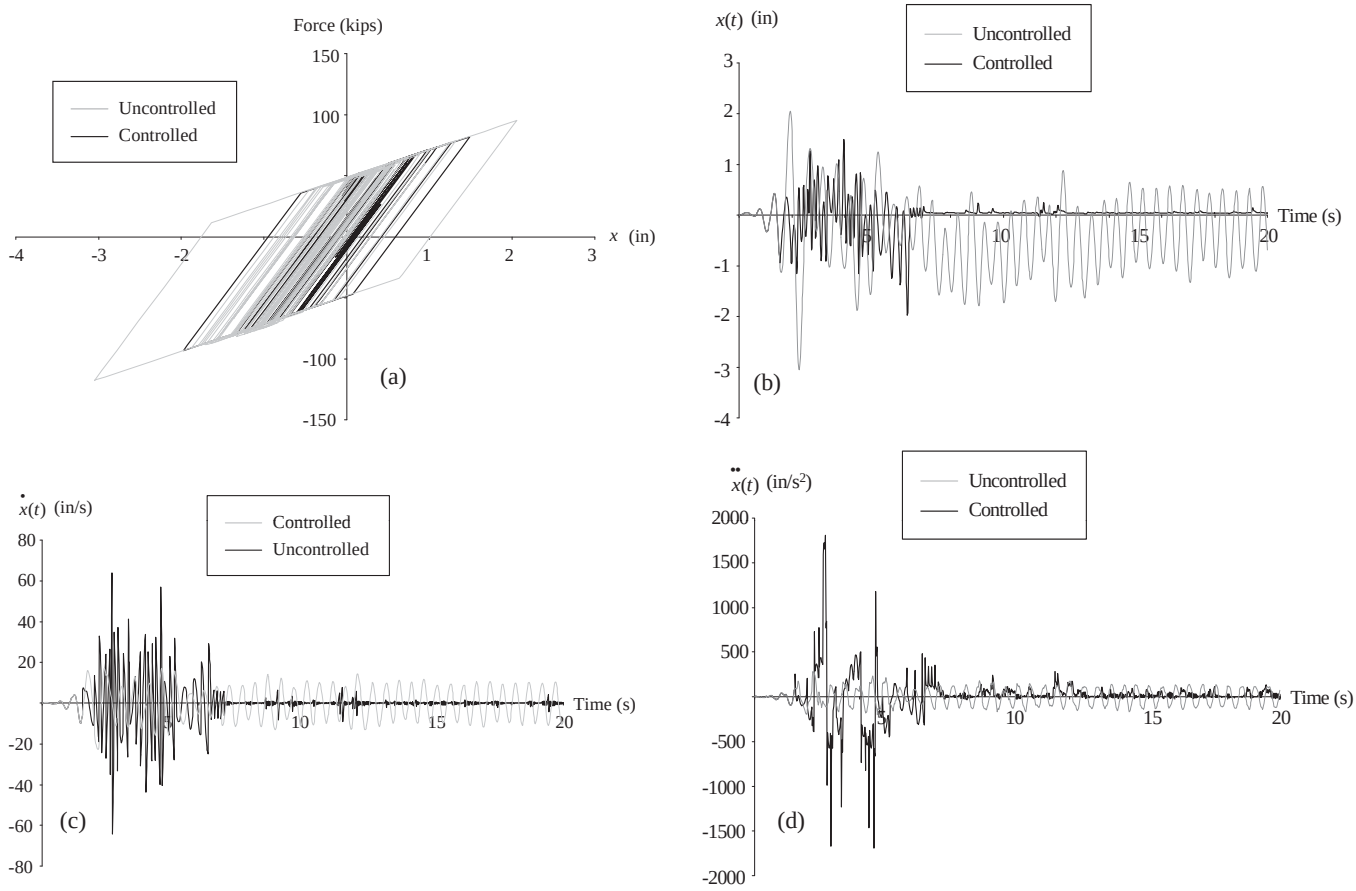

Figure 15. Responses using an evolutionary gain and the absolute-Z approach, with a strain-based performance objective of 125% of the yield deflection (0.8805 in): (a) force-displacement hysteresis; (b) displacement time history; (c) velocity time history; (d) acceleration time history.

reduction in deflection in addition to the amount of strain energy being dissipated, which is calculated as 71% less for this controlled system than for the uncontrolled system. Although the system produces dramatic improvement in the prevention of structural damage compared to the control system that uses the displacement-based performance objective (Figure 13), the velocity and acceleration time histories are greater than those for the uncontrolled system in the first few seconds of the response but are smaller for the majority of the response history; see Figures 15c,d.

Figures 16a–e show the responses using a strain-based performance objective and forcing the system to yield. Figure 16a shows the force-deflection hysteresis of the forced- and not forced-to yield responses, where the former are visibly smaller. The strain energy dissipation when forcing the system to yield dramatically reduces the amount of damage, if measured in terms of the dissipated strain energy, wherein strain energy decreases by 95% compared to the uncontrolled system and by 82% when compared to the system that is not forced to yield. Examining the time histories (parts b–e of Figure 16), it is again apparent that forcing the system to yield decreases the velocity and acceleration, and decreases the amount of control force required to manage the system. A comparison of Figures 13a, 14a, 15a, and 16a shows that

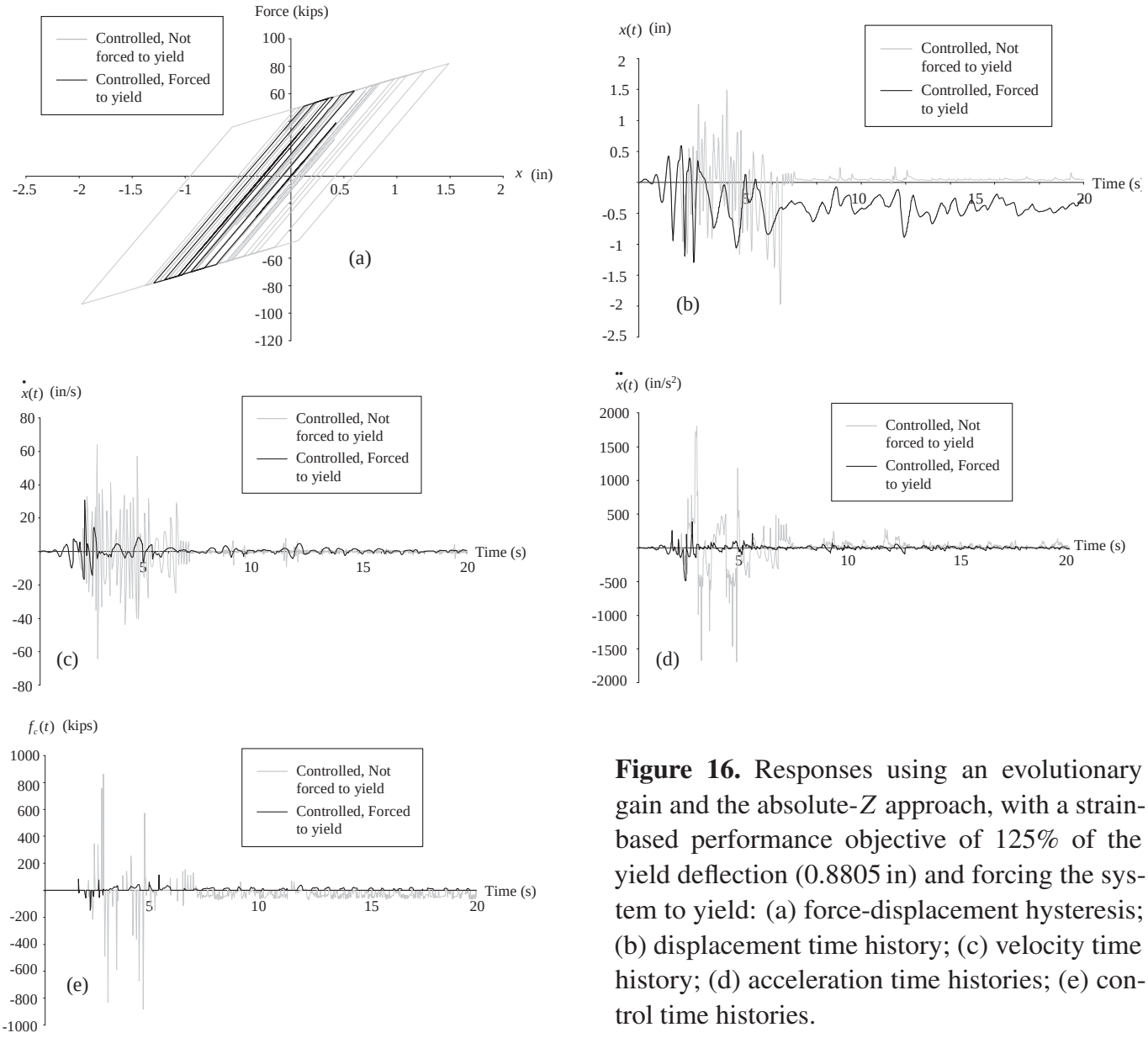

Figure 16. Responses using an evolutionary gain and the absolute-Z approach, with a strain-based performance objective of 125% of the yield deflection (0.8805 in) and forcing the system to yield: (a) force-displacement hysteresis; (b) displacement time history; (c) velocity time history; (d) acceleration time histories; (e) control time histories.

for the absolute-Z approach, the most optimal control solution for minimizing inelastic damage includes using a strain-based performance objective where the system is forced to yield in the as-needed condition and using an evolutionary gain formulation.

Figure 17 shows the responses using a delta-Z approach and a displacement-based performance objective. In Figure 17a we see the force-deflection hysteresis versus that of the uncontrolled system, where the controlled system does not even complete a full hysteresis loop during the tested duration of the earthquake. This implies that there is no same-side reyielding and results in strain energy dissipation that is 99% less than that of the uncontrolled system. The time histories in the remaining parts of Figure 17 reveal that the velocity and acceleration are also reduced, where the maximum acceleration is 34% less than that of the uncontrolled system. The magnitude of the control force (Figure 17e) is only 58 kips, but it is applied more frequently than in the displacement-based cases. This implies that smaller, more

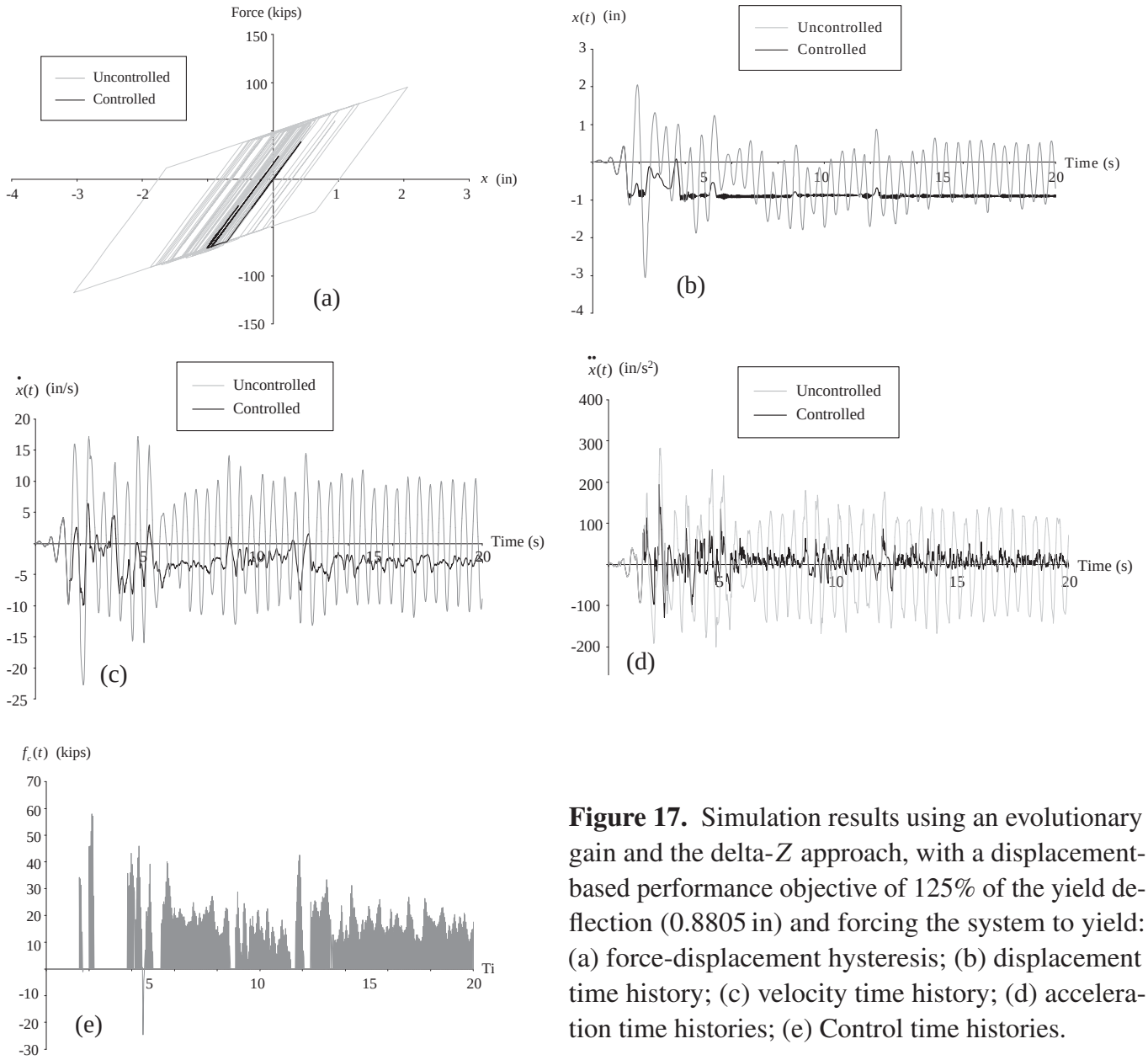

Figure 17. Simulation results using an evolutionary gain and the delta-Z approach, with a displacement-based performance objective of 125% of the yield deflection (0.8805 in) and forcing the system to yield: (a) force-displacement hysteresis; (b) displacement time history; (c) velocity time history; (d) acceleration time histories; (e) Control time histories.

cost-effective devices may be used to control the system using this method of control, but physically, they may be required to apply new control forces at each time step.

Using a strain-based performance objective, the force-deflection hysteresis is nearly the same as that in Figure 17a. Further, the dissipated strain energy is nearly identical for both the displacement-based and strain-based systems, as are the velocity and acceleration time histories, and as is the control force time-history, which has a maximum of 60 kips in this case. Therefore, it is evident that the selection of the performance objective (strain-based versus displacement-based), has virtually no influence when using the delta-Z approach since, as mentioned earlier, that small quantities of energy are utilized in the cost function minimization due to the delta formulation; see (21).

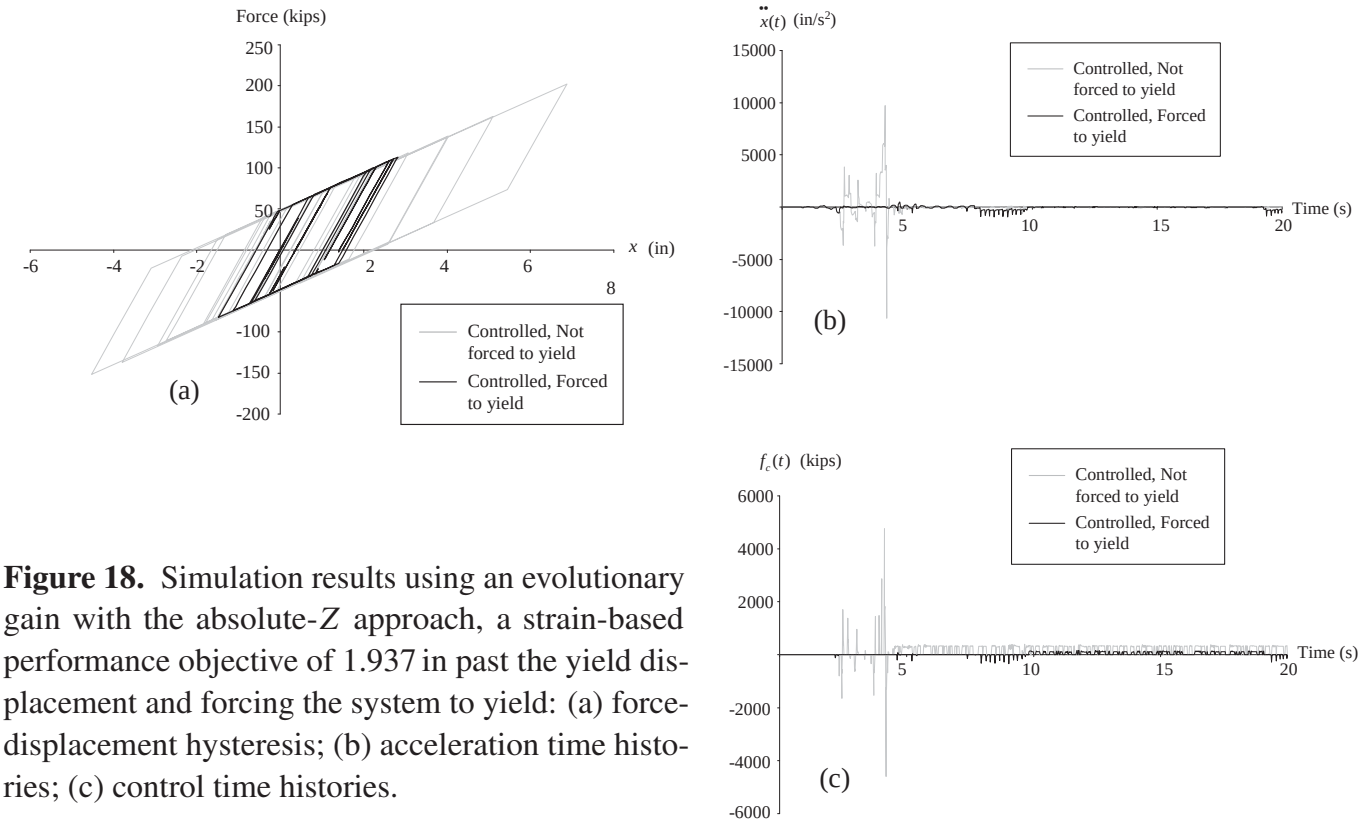

Figure 18. Simulation results using an evolutionary gain with the absolute-Z approach, a strain-based performance objective of 1.937 in past the yield displacement and forcing the system to yield: (a) force-displacement hysteresis; (b) acceleration time histories; (c) control time histories.

Investigation 2. The next investigation allows significantly more damage to occur in members; that is, a lower performance objective is demanded. Figure 18a shows the force-deflection hysteresis when the absolute-Z approach is applied to a system that is forced to yield and used in conjunction with a strain-based performance objective (set to 375% of the first-yield displacement in Investigation 2, or 1.937 inches past yield; see Table 2). The results are favorable; we see a considerable decrease in the size of the hysteresis loops when the system is forced to yield (as opposed to not being forced to yield) and a maximum displacement of 2.55 in. The maximum displacement of the uncontrolled system was 3.05 in. (Figure 8a) and the resulting strain energy dissipation is 46% less than that of the uncontrolled system. However, the maximum acceleration (Figure 18b) was 2.46 g's, which was approximately 10% of the maximum acceleration in the unforced system, but still 3.37 times the maximum acceleration seen in Figure 8d (page 871) for the uncontrolled system. Figure 18c compares the control force time histories of the forced and unforced systems, where the former is clearly favorable.

The delta-Z approach was then applied to a not-forced-to-yield system in an effort to reduce the necessary control force and subsequent energy input to the single-DOF system so that responses may be minimized while the responses remained stable; Figure 19 shows the results for both the displacement-based system (left column) and the strain-based system (right column). The delta-Z approach significantly reduced the number of cycles in the force-deflection hysteresis (top row of Figure 19) compared to that of the uncontrolled system (Figure 8a), resulting in a 79% decrease (displacement-based) and a 84% decrease (strain-based) in the dissipated strain energy. The maximum accelerations (middle row of Figure 19) were found to be 0.84 g's and 0.65 g's for the displacement-based and strain-based systems, respectively, whereas the uncontrolled system's maximum acceleration was 0.73 g's (Figure 8d). The

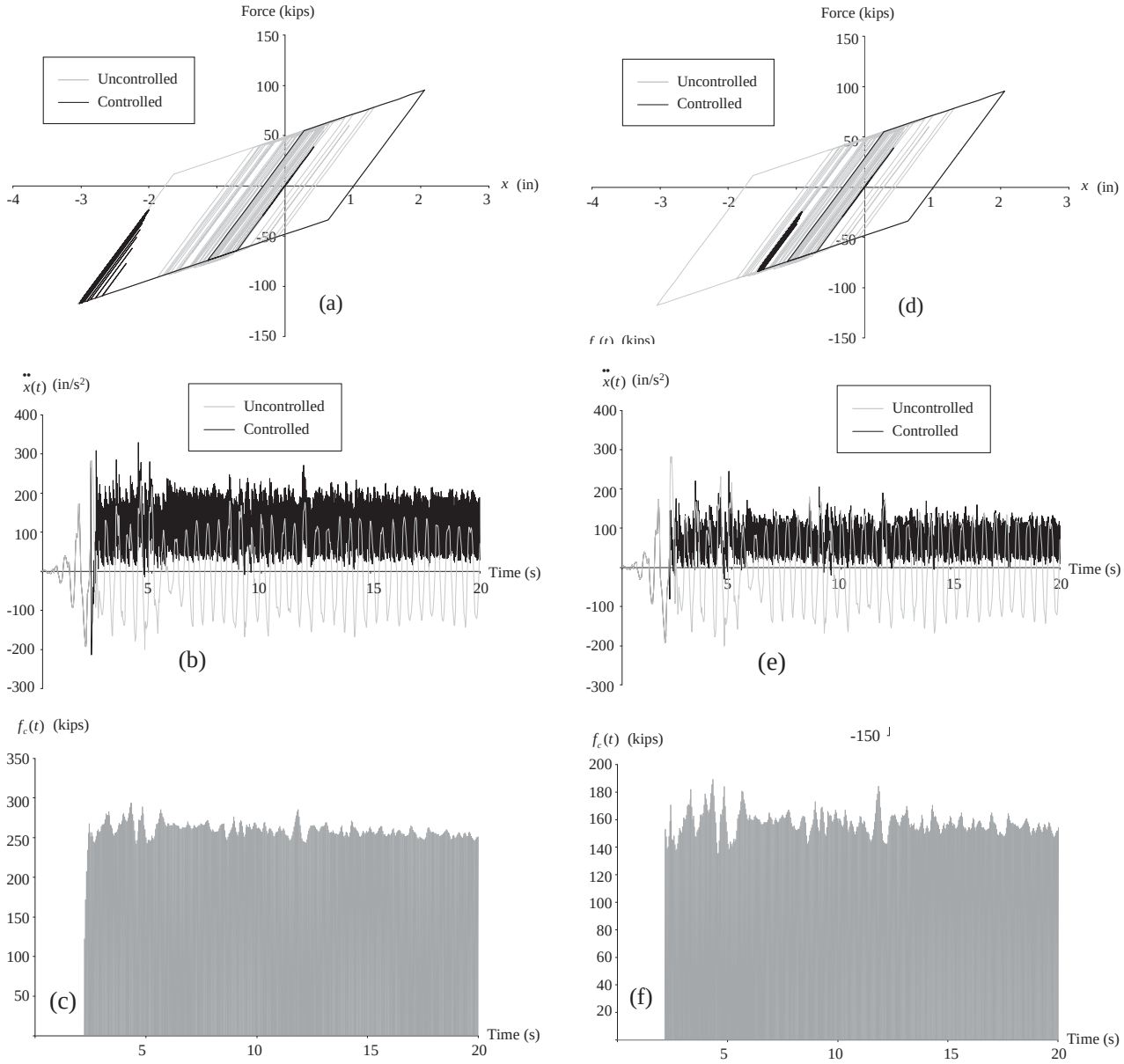

Figure 19. Left column: force-deflection hysteresis, acceleration, and control force obtained using evolutionary gain as part of the delta-Z approach with a displacement-based performance objective of 375% of the yield deflection, or 2.64 in. Right column: corresponding quantities obtained with a strain-based performance objective consisting of a post-yield strain of 2.75 times $\varepsilon_{\text{yield}}$, or a post-yield deflection of 1.94 in.

abrupt changes in the accelerations after 2.4 seconds were caused by the sudden application of control forces after 2.38 seconds — this in response to the system trying to reverse its direction after 2.38 seconds, as shown by the same-side reyielding of the force-displacement hysteresis in quadrant 3 in both cases.

The bottom row of Figure 19 shows the control force distributions for the displacement-based and strain-based systems; the maximum control forces are 298 kips and 190 kips, respectively. A comparison

Conditions			Experiment 1				Experiment 2			
			change in strain energy dissipation	maximum structure acceleration (in/s^2)	change in maximum acceleration	maximum control force	change in strain energy dissipation	maximum structure acceleration (in/s^2)	change in maximum acceleration	maximum control force
A	D	N	264%	3000	900%	1500	2536%	8000	2567%	3500
A	D	Y	−20%	2000	567%	800	25%	800	167%	450
A	S	N	−71%	1800	500%	900	207%	10000	3233%	5000
A	S	Y	−95%	500	67%	100	−46%	950	217%	350
Δ	D	N	−99%	200	−33%	60	−76%	325	8%	300
Δ	S	N	−99%	200	−33%	60	−84%	250	−17%	190

Table 3. Summary of evolutionary gain results for controlling inelastic damage, with percent changes relative to the uncontrolled situation. The first code under "Conditions" indicates the approach (absolute-Z or delta-Z), the second the type of performance objective (displacement-based or strain-based), and the third whether or not the member is forced to yield. The best results are highlighted.

of the two indicates that the latter is clearly capable of controlling already-damaged systems while reducing accelerations using a moderate level of control force.

Summary of as-needed approaches for inelastic control. A summary of the two investigations is shown in Table 3 using the six combination of conditions listed on page 872. In each investigation, the delta-Z approach proved to be more capable of controlling the amount of strain energy being dissipated (and henceforth limit the amount of permanent damage) in the members and reduce the accelerations than the absolute-Z approach.

Table 3 shows that by utilizing a strain-based performance objective, the delta-Z approach provides the optimal evolutionary control strategy where there is 99% reduction in structural damage and a 33% reduction in the maximum acceleration compared to the uncontrolled system in Investigation 1 while requiring a maximum control force of only 60 kips. In Investigation 2, which employed a lower performance objective (hence more allowable damage — damage of 2.75 times the yield response), there was an 84% decrease in damage and a 17% decrease in the maximum acceleration, with a still-moderate control force of 190 kips.

6. Conclusions

A linear optimal control solution for controlling inelastic and elastic systems using an evolutionary gain and a state-space transition formulation is presented. Control forces may be generated and applied during each time step in order to satisfy required performance objectives, which may be defined either globally

with respect to the original equilibrium position of the member, or locally with respect to the current yield position of the member during each cyclic response. The elastic and inelastic response components of the simulated responses are separated based on the discretized plastic excursions of the degrading system. A kinematically strain-hardening assumption is used to define the hysteresis of the material as it unloads, reyields, and reloads. A computer program, CONON (for control nonlinear time-history analysis) was developed herein to simulate and control the inelastic responses in shear frames using the proposed evolutionary gain approach. The code uses an efficient subroutine to expeditiously converge to the desired performance objectives. It was found that the procedure was able to adequately converge to the desired performance objectives for an earthquake excitation using a minimal amount of control force while alleviating the dependence on weighing matrices that might inconsistently satisfy or not satisfy performance objectives and result in excessive and costly output control forces.

Further, the delta-Z approach used in conjunction with a strain-based performance objective was found to be the optimal solution in effectively mitigating damage (measured in terms of strain energy dissipation), which was reduced by at least 84%, and in effectively reducing the overall maximum acceleration by at least 17%. In addition, the delta-Z approach also required the smallest amount of control force, which indicated that developing such an optimal evolutionary controller may also present the cheapest solution. Nonetheless, the absolute-Z approach was also able to effectively reduce the strain energy dissipation in the two investigations when used in conjunction with a strain-based performance objective and when the system was forced to yield.

References

[Agrawal and Yang 2000] A. K. Agrawal and J. N. Yang, "Compensation of time-delay for control of civil engineering structures", *Earthquake Eng. Struct. Dyn.* **29**:1 (2000), 37–62.

[Attard 2005] T. L. Attard, "Post-yield material nonlinearity: optimal homogeneous shear-frame sections and hysteretic behavior", *Int. J. Solids Struct.* **42**:21–22 (2005), 5656–5668.

[Attard and Dansby 2008] T. L. Attard and R. E. Dansby, "Evolutionary control of damaged systems using a rehabilitative algorithm", in *Tenth Pan American Congress of Applied Mechanics* (*PACAM X*) (Cancún, 2008), vol. 12, edited by T. L. Attard, 2008. To appear.

[Attard and Mignolet 2005] T. L. Attard and M. P. Mignolet, "Evolutionary model for random plastic analyses of shear-frame buildings using a detailed degradation model", pp. 533–540 in *Safety and reliability of engineering systems and structures: proceedings of the* 9^{th} *International Conference on Structural Safety and Reliability* (*ICOSSAR 2005*) (Rome, 2005), edited by G. Augusti et al., Millpress, Rotterdam, 2005.

[Attard and Mignolet 2008] T. L. Attard and M. P. Mignolet, "Random plastic analysis using a constitutive model to predict the evolutionary stress-related responses and time passages to failure", *J. Eng. Mech.* (*ASCE*) **134**:10 (2008), 881–891.

[Attard et al. 2009] T. L. Attard, R. E. Dansby, and M. Marusic, "Optimal nonlinear structural damage control for kinematically strain hardened systems using an evolutionary state transition", in *Computational structural dynamics and earthquake engineering, COMPDYN 2007* (Rethymno, 2007), edited by M. Papadrakakis et al., Structures and Infrastructures **2**, Taylor and Francis, London, 2009.

[Caughey 1998] T. K. Caughey, "The benchmark problem", *Earthquake Eng. Struct. Dyn.* **27**:11 (1998), 1125.

[Christenson and Emmons 2005] R. E. Christenson and A. T. Emmons, "Semiactive structural control of a nonlinear building model: considering reliability", in *Metropolis and beyond: proceedings of the 2005 Structures Congress and the 2005 Forensic Engineering Symposium* (New York, 2005), ASCE, Reston, VA, 2005.

[Conner 2003] J. J. Conner, *Introduction to structural motion control*, Prentice Hall, Upper Saddle River, NJ, 2003.

[FEMA 2001] "The 2000 NEHRP recommended provisions for seismic regulations for new buildings and other structures, 1: Provisions", FEMA Report 368, Building Seismic Safety Council/Federal Emergency Management Agency, Washington, DC, 2001, Available at http://www.bssconline.org/NEHRP2000/comments/provisions.

[Franklin et al. 2002] G. F. Franklin, J. D. Powell, and A. Emami-Naeini, *Feedback control of dynamic systems*, Prentice Hall, Upper Saddle River, NJ, 2002.

[Gavin et al. 2003a] H. P. Gavin, C. Alhan, and N. Oka, "Fault tolerance of semiactive seismic isolation", *J. Struct. Eng.* (*ASCE*) **129**:7 (2003), 922–932.

[Gavin et al. 2003b] H. P. Gavin, P. Phule, and A. Jones, "Design optimization of MR devices and materials", in *Proceedings of the 3rd World Conference on Structural Control* (*3WCSC*) (Como, 2002), edited by F. Casciati, Wiley, Chichester, 2003.

[Gavin et al. 2003c] H. P. Gavin, J. Thurston, A. Singer, H. Fujitani, and C. Minowa, "Effects of damper force ranges and ground motion pulse periods on the performance of semi-active isolation systems", pp. 79–85 in *Problems involving thermal hydraulics, liquid sloshing, and extreme loads on structures* (Cleveland, OH, 2003), edited by F. J. Moody et al., PVP **454**, ASME, New York, 2003. Paper No. PVP2003-1819.

[Hart and Wong 2000] G. C. Hart and K. K. F. Wong, *Structural dynamics for structural engineers*, Wiley, New York, 2000.

[Howard et al. 2005] J. K. Howard, C. A. Tracy, and R. G. Burns, "Comparing observed and predicted directivity in near-source ground motion", *Earthquake Spectra* **21**:4 (2005), 1063–1092.

[IBC 2003] *International building code*, International Code Council, Country Club Hills, IL, 2003.

[Kelly 1999] J. M. Kelly, "The role of damping in seismic isolation", *Earthquake Eng. Struct. Dyn.* **28**:1 (1999), 3–20.

[Kim and Adeli 2004] H. Kim and H. Adeli, "Hybrid feedback-least square algorithm for structural control", *J. Struct. Eng.* (*ASCE*) **130**:1 (2004), 120–127.

[Lemaitre and Chaboche 1990] J. Lemaitre and J. L. Chaboche, *Mechanics of solid materials*, Cambridge University Press, Cambridge, 1990.

[Madden et al. 2002] G. J. Madden, M. D. Symans, and N. Wongprasert, "Experimental verification of seismic response of building frame with adaptive sliding base-isolation system", *J. Struct. Eng.* (*ASCE*) **128**:8 (2002), 1037–1045.

[Makris 1997] N. Makris, "Rigidity-plasticity-viscosity: can electrorheological dampers protect base-isolated structures from near-source ground motions?", *Earthquake Eng. Struct. Dyn.* **26**:5 (1997), 571–591.

[Nagarajaiah and Mao 2004] S. Nagarajaiah and Y. Mao, "Response of smart base isolated structures with independently variable stiffness and variable damping systems in near fault earthquakes", in *Proceedings of the US-Korea Joint Seminar/Workshop on Smart Structures Technologies* (Seoul, 2004), edited by C.-B. Yun and L. A. Bergman, Techno-Press, Daejeon, 2004.

[Nagarajaiah et al. 2000] S. Nagarajaiah, S. Sahasrabudhe, and R. Iyer, "Seismic response of sliding isolated bridges with smart dampers subjected to near source ground motions", Chapter 1, Section 5 , in *Advanced technology in structural engineering: Structures Congress 2000* (Philadelphia, 2000), edited by M. Elgaaly, ASCE, Reston, VA, 2000.

[Nagarajaiah et al. 2004] S. Nagarajaiah, A. Agrawal, and E. Sonmez, "Response of SDOF systems with variable stiffness and damping systems to pulse type of excitations", in *Proceedings of the* 3^{rd} *International Conference on Earthquake Engineering* (*3ICEE*)*: new frontier and research transformation* (Nanjing, 2004), edited by W. Liu et al., China Water Power Press, Beijing, 2004.

[Ohtori et al. 2004] Y. Ohtori, R. E. Christenson, B. F. Spencer, Jr., and S. J. Dyke, "Benchmark control problems for seismically excited nonlinear buildings", *J. Eng. Mech.* (*ASCE*) **130**:4 (2004), 366–385.

[Ragab and Bayoumi 1999] A. Ragab and S. E. Bayoumi, *Engineering solid mechanics: fundamentals and applications*, CRC Press, Boca Raton, FL, 1999.

[Reynolds and Christenson 2006] W. E. Reynolds and R. E. Christenson, "Bench-scale nonlinear test structure for structural control research", *Eng. Struct.* **28**:8 (2006), 1182–1189.

[Ribakov 2004] Y. Ribakov, "Semi-active predictive control of non-linear structures with controlled stiffness devices and friction dampers", *Struct. Des. Tall Spec. Build.* **13**:2 (2004), 165–178.

[Symans and Reigles 2004] M. D. Symans and D. G. Reigles, "Supervisory fuzzy logic control of smart seismic isolation systems", in *Building on the past, securing the future: proceedings of the 2004 Structures Congress* (Nashville, TN, 2004), edited by G. E. Blandford, ASCE, Reston, VA, 2004.

[Varadarajan and Nagarajaiah 2004] N. Varadarajan and S. Nagarajaiah, "Wind response control of building with variable stiffness tuned mass damper using empirical mode decomposition/Hilbert transform", *J. Eng. Mech.* (*ASCE*) **130**:4 (2004), 451–458.

[Wong 2005a] K. K. F. Wong, "Predictive optimal linear control of elastic structures during earthquake, I", *J. Eng. Mech.* (*ASCE*) **131**:2 (2005), 131–141.

[Wong 2005b] K. K. F. Wong, "Predictive optimal linear control of inelastic structures during earthquake, II", *J. Eng. Mech.* (*ASCE*) **131**:2 (2005), 142–152.

[Wong and Yang 2002] K. K. F. Wong and R. Yang, "Earthquake response and energy evaluation of inelastic structures", *J. Eng. Mech.* (*ASCE*) **128**:3 (2002), 308–317.

[Wu 2005] H. C. Wu, *Continuum mechanics and plasticity*, Chapman and Hall/CRC Press, Boca Raton, FL, 2005.

[Yang et al. 1990] J. N. Yang, A. Akbarpour, and G. Askar, "Effect of time delay on control of seismic-excited buildings", *J. Struct. Eng.* (*ASCE*) **116**:10 (1990), 2801–2814.

[Yang et al. 1996] J. N. Yang, J. C. Wu, and Z. Li, "Control of seismic-excited buildings using active variable stiffness systems", *Eng. Struct.* **18**:8 (1996), 589–596.

[Zhang and Iwan 2002] Y. Zhang and W. D. Iwan, "Active interaction control of tall buildings subjected to near-field ground motions", *J. Struct. Eng.* (*ASCE*) **128**:1 (2002), 69–79.

[Zhou et al. 2003] L. Zhou, C.-C. Chang, and L.-X. Wang, "Adaptive fuzzy control for nonlinear building-magnetorheological damper system", *J. Struct. Eng.* (*ASCE*) **129**:7 (2003), 905–913.

Received 19 Jan 2009. Revised 16 May 2009. Accepted 16 May 2009.

THOMAS L. ATTARD: tattard@utk.edu
Department of Civil and Environmental Engineering, The University of Tennessee, 113 Perkins Hall, Knoxville, TN 37996-2010, United States

ROBIN E. DANSBY: rdansby@csufresno.edu
California State University, Fresno, Department of Civil and Geomatics Engineering, M/S EE94, 2320 E. San Ramon Avenue, Fresno, CA 93740-8030, United States